Chapter 8

Wheeler's delayed-choice thought experiment with a single atom

Broadly speaking, the delayed-choice experiments in quantum mechanics deal with a situation in which the observer chooses to reveal the particle or wave character of a quantum system at a later stage of the experiment. These experiments are attempts to demonstrate whether the particle somehow "senses" the experimental apparatus it will interact with and adjusts its behaviour (wave-like or particle-like) accordingly, by assuming the appropriate determinate state for it, or whether the particle remains in an indeterminate state: neither wave nor a particle.

Delayed-choice experiments have particularly highlighted certain peculiarities and non-classical features. In interferometric delayed-choice experiments, the choice whether to observe the particle or wave character of a quantum object can be delayed with respect to the object entering the interferometer. Moreover, it is possible to observe a continuous transformation between these two extreme cases. This rules out the naive classical interpretation that every quantum system behaves either definitely as a particle or definitely as a wave by adapting a priori to the specific experimental situation [142].

Wheeler's thought experiment is important since it tries to force a classical view of reality on to a quantum system. If one holds the view that in order to observe interference at the detector the photon must have traversed both arms (as a wave) of the interferometer (and conversely that the lack of interference unambiguously demonstrates the photon traversed a single arm (as a particle)) then the "delayed" choice creates a conundrum. In this picture, the choice of detection (delayed until after the photon has passed the first beamsplitter) is correlated with observing interference or no interference – and thus it appears that a future event (the method of detection) causes the photon to decide its past. If such a perspective seems untenable with a fast moving massless photon, then our experiment, which uses a slow moving massive helium atom (and thus is closer to our classical notions) makes this view of reality seem even more unlikely.

Here, we report the first realization of Wheeler's famous delayed choice *gedankenexperiment* with single massive particles. The only successful demonstration of Wheeler's ideas to date has been achieved with single photons [82]. Here we use atoms, which is an important distinction, since atoms have many internal degrees of freedom. This allows coupling to the external environment through, for example the atom's sensitivity to magnetic and electric fields. Moreover, an atom has significant mass which allows strong coupling to gravitational fields. These interactions of the atom with its environment are required for the appearance of decoherence and thus in this sense an atom can be thought of as a more classical particle than a photon. As such, our experiment tests

Wheeler's ideas in a regime in which it has never been tested.

In our realization of the experiment, we apply a Mach-Zehnder interferometer to a single ultracold metastable helium atom to demonstrate an atomic analogue of Wheeler's original proposal. Our measurements confirm Bohr's view that it does not make sense to ascribe a wave or particle behaviour to a massive particle until a measurement occurs [143]. This result is encouraging for current work towards entanglement and Bell's theorem tests in macroscopic systems of massive particles [144].

The findings presented in this chapter have resulted in the publication:

[4] A. G. Manning, R. I. Khakimov, R. G. Dall, and A. G. Truscott. "Wheeler's delayed-choice gedanken experiment with a single atom". *Nature Physics* 11 (2015), 539

8.1 Overview

The development of quantum mechanics has revolutionised our understanding of the physical world, and introduced many counter-intuitive notions. Among the most fundamental is that we have to consider light and matter as both waves and particles, and that the nature of the measurements we make influences which of those two seemingly incompatible behaviours we observe. A striking example of this was conceived by Wheeler in his famous "delayed choice" *gedankenexperiment* [143], recently demonstrated with single photons [82]. A comprehensive overview of the topic can be found in the recent review [142].

The question of whether light behaves like a particle or wave has had a long and strongly contested history until the advent of quantum mechanics, where it was accepted that it could indeed display either behaviour (Fig. 8.1). Conversely, it was de Broglie's hypothesis of matter waves [145] that deviated from the preceding view of massive bodies exclusively as particles, which was confirmed by the electron diffraction experiments of Davisson and Germer [146]. Even more bizarrely, the way in which an experiment is performed appears to induce one of these behaviours at the exclusion of the other. The question of whether a single photon in an interferometer passes through either one arm (as a particle) or both simultaneously (as a wave) led to Wheeler devising his famous *gendankenexperiment*, which supposed that the decision of whether to attempt to measure particle or wave behaviour is made after the photon enters the interferometer. By removing the second beamsplitter of the interferometer (Fig. 8.2(A)), which way information is revealed [147], which precludes an interference measurement, while inserting the beamsplitter destroys information about the path taken by the photon and re-establishes a wave interference dependent on the phase difference between the arms.

Although many experiments have shown particle-wave duality with photons [142], including delayed choice schemes [148–150], delayed choice quantum eraser experiments [151] and entanglement swapping utilizing delayed choice [152], only recently has the complete scheme proposed by Wheeler been realised experimentally by Jacques *et al* [82]. By simultaneously ensuring that only a single photon is present in the interferometer at once, and that the decision of interferometer configuration is relativistically separated from the photon's entry to the interferometer, it was unambiguously shown that Wheeler's supposition that such a choice affects the "past history" of the photon was correct.

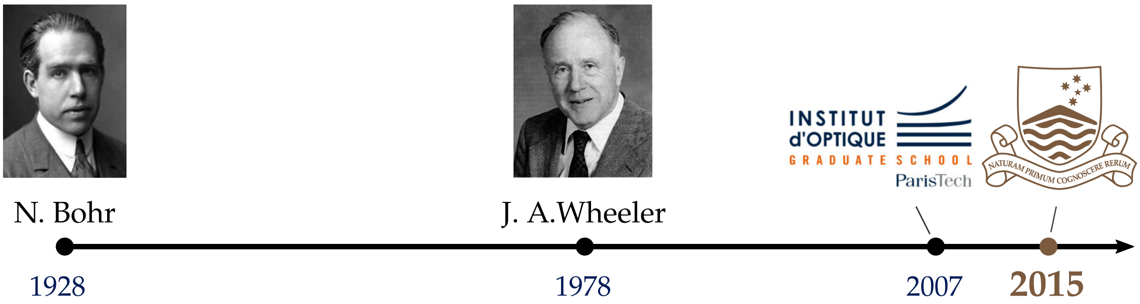

Figure 8.1: Timeline of the Wheeler's idea development.
1928 – Bohr's complementarity principle;
1978 – Wheeler's thought experiment: wave or particle?
2007 – First experiment with a single photon [82];
2015 – First experiment with a single atom (this work).

Recent advances in the trapping and cooling of atoms has led to the ability to readily observe wavelike phenomena with particles that have mass, such as the interference between two Bose – Einstein condensates [153]. However, progress towards demonstrating Wheeler's experiment with massive particles, such as a delayed choice Stern-Gerlach interferometer with metastable hydrogen [154] or a spin interferometer with neutrons [155], have been limited. Some previous attempts include experiment with metastable argon atoms [156], similar in its idea to our implementation. Importantly, these experiments used beams containing more than one particle in the apparatus at any one time rendering a meaningful test of Wheeler's ideas impossible, at least at the quantum level. Nonetheless, they demonstrate an advantage of using massive particles over photons, the relatively slow velocity (compared to light) of the atoms through the interferometer allows an increased time for making the delayed choice.

8.1.1 Atomic version of the the experiment: a general overview.

Before proceeding to a technical description of the experimental method, a brief conceptual overview will be given here. We use an ultracold (<1nK) source of single atoms (see Chapter 4 and Ref. [7]) to implement Wheeler's idea: that the behaviour of the atom can indeed be induced by our choice of measurement. Our experimental setup closely mirrors that of the Mach-Zehnder scheme originally proposed by Wheeler (Fig. 8.2), where essentially the roles of light and matter have been reversed. Atoms are released from an optical dipole trap and fall under gravity towards the detector.

About 1 ms after releasing the atoms from the trap, a pair of laser beams are used to Bragg scatter the atoms into different momentum modes [20], where a Bragg pulse of duration T_π coherently transfers from one momentum mode to another in a two state system [10], and a pulse duration $T_{\pi/2}$ transfers one momentum mode into an equal superposition of the two modes. The action of a π pulse is thus analogous to a mirror, while the $\pi/2$-pulse acts as a 50:50 beamsplitter. An arbitrary phase can be applied to the atomic wavefunction by controlling the phase of the Bragg pulses. In particular, we set the phase to zero for all pulses except for the first $\pi/2$ pulse, which carries an adjustable relative phase ϕ. After applying the π-pulse, a quantum random bit generator is triggered to decide whether the second $\pi/2$-pulse should be initiated, which is equivalent to the addition or removal of the second beamsplitter in the optical case (Fig 8.2). In our experiment, we use Bragg pulses of order of tens of μs (and a $\pi/2 - \pi/ - \pi/2$ sequence

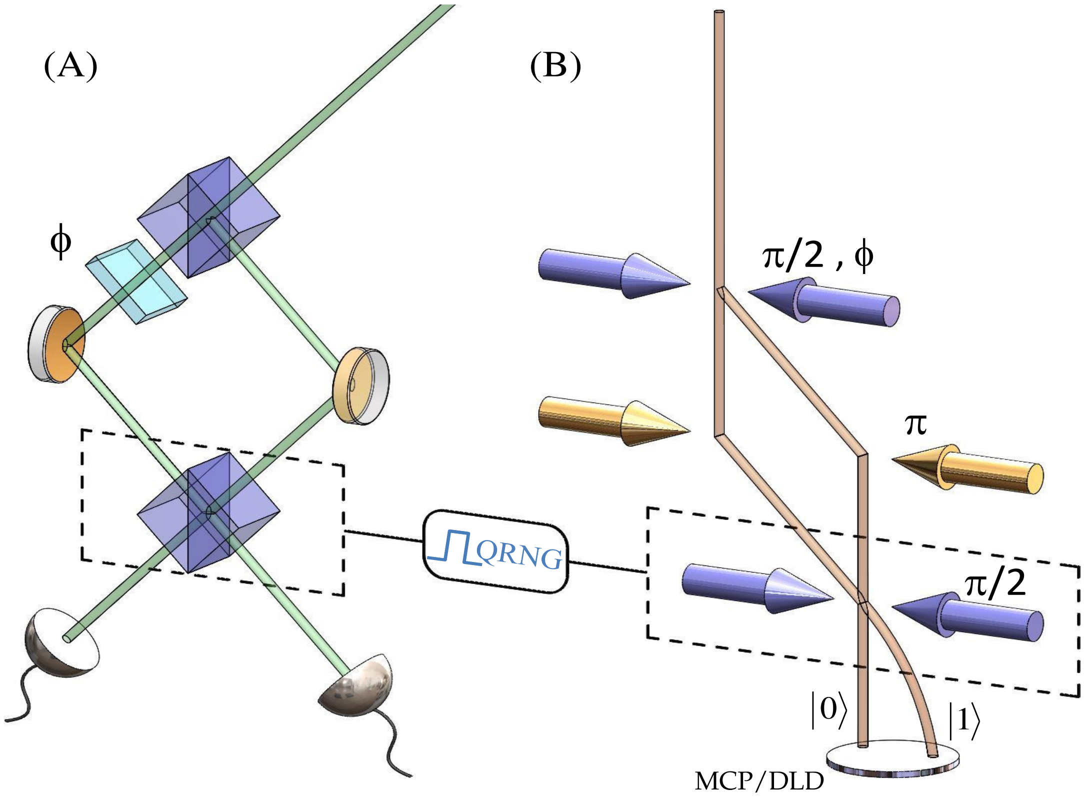

Figure 8.2: Schematic of the Wheeler's experiment. (A) Optical version of Wheeler's delayed choice experiment. **(B)** Atomic version of experiment, where the physical beamsplitters and mirrors are now replaced with optical Bragg pulses. A quantum random number generator (QRNG) is used to decide whether the last beamsplitting pulse is either implemented or not. The random number is triggered and chosen after the Bragg π-pulse (mirror pulse). This ensures that as it enters the interferometer, the atom has no prior knowledge of how it will be detected. A relative phase ϕ between the two modes of the atomic wavefunction is imprinted with the first $\pi/2$-pulse, and after applying the π-pulse (mirror), a decision is made whether to apply the final $\pi/2$-pulse to mix the arms of the interferometer. After this process, the two momentum modes separate during the time of flight to the detector (MCP/DLD), where they arrive spatially and temporally separated. The probability of a count arriving in either location of the DLD is then either dependent on the phase ϕ (if the final $\pi/2$-pulse is applied), or otherwise will be independent of ϕ.

of hundreds of μs duration) and generate the random bit and implement its result 170 μs after the first beamsplitting pulse (when the atom is half way through the interferometer), thus ensuring that the choice of detection is made well after the atom passes the first beamsplitter, and thus the atom has no "prior knowledge" about the final configuration of the interferometer.

If the second $\pi/2$-pulse is applied, then the arms of the interferometer are mixed, and the relative phase between the arms ϕ generated at the first beamsplitter, can affect the probability of each atom being in a given momentum mode. Should this pulse be disabled, then there is a 50% chance that the atom will travel down either path of the interferometer in the "open" configuration, which means that the average count rate for each momentum mode will be 50% irrespective of the phase ϕ applied. Instead of having a separate detector to measure counts in each arm of the interferometer, we can easily resolve the two momentum modes due to their arrival at different spatial positions and times on the same MCP/DLD [81].

The delayed choice of whether the second $\pi/2$-pulse is present to mix the arms of the interferometer must be made randomly and relativistically separated from the entry of the atom to the interferometer, to exclude justifications for the experimental result which invoke Einstein's argument of local reality. While this aspect of the experiment is challenging for photons travelling at the speed of light, this is straightforward for atoms moving at speeds no greater than a few metres per second. Commercially available quantum random number generators (QRNG) are capable of producing the random choice on a microsecond time scale, which is sufficient for setting the interferometer configuration after the *pi*-pulse is applied by triggering a switch which enables/disables the final $\pi/2$-pulse. The state of the switch can also be recorded so that the two configurations can be distinguished after each experimental iteration at the data post-processing stage.

8.2 Experimental method

There are two main components to our realization of the Wheeler's experiment:

- a source capable of producing at most one atom at a time, and
- an atom interferometer with a programmable final beamsplitter, which can be switched on and off at random, after the atom has passed a first beamsplitter.

The development of a single atom source is described previously in Chapter 4, therefore in the following we focus mainly on implementation of the interferometer, providing only a summary of the results regarding the source which are relevant to this experiment.

8.2.1 Single atom source

The experimental setup (Fig. 8.3) is largely based on [65, 92]. Ultracold ^{4}He* is magnetically trapped and evaporatively cooled [141] to just below the BEC transition temperature (~ 1 μK). Around 10^4 atoms are transferred into a vertical optical dipole trap by ramping up the intensity of a far red detuned focused laser beam in the direction of gravity over 200 ms. The magnetic trap is switched off and the only magnetic field present is generated by our magnetic field stabilisation "nullerometer" [93], which provides a bias magnetic field ~1 Gauss. Then, the dipole trap is ramped down over 100 ms, resulting in a trap with harmonic frequencies of $(\omega_z, \omega_y, \omega_z)/2\pi = (1800, 1800, 12)$ Hz. The trap depth (equivalent to a temperature of a few nanokelvin) is then held at this point for two seconds, which allows the majority of the thermal atoms to exit the trap.

To obtain a single atom source [7], we induce Penning ionization losses in the cloud described above by spin flipping the atoms from the $m_J = +1$ state to the $m_J = 0$ state with RF radiation, which increases the rate of two body Penning ionization loss by ~5 orders of magnitude [157]. The two body collisional lifetime of $m_J = 0$ atoms in our dipole trap is ($\sim$10 ms), which is much shorter than the lifetime of $m_J = +1$ atoms in the same trap ($\sim$25 s) or the radiative lifetime of the metastable helium excited state (7870 s [84]). By holding the $m_J = 0$ atoms for 5 s we obtain a single atom in 50% of experimental cycles, and no atoms otherwise, depending on whether we start with an odd or even number of atoms in the trap respectively. As each experimental cycle represents obtaining a single atom (or lack thereof), we are able to determine (with reference to detector efficiency $\sim$ 20% and trap lifetime) that we only have at most a single atom present with

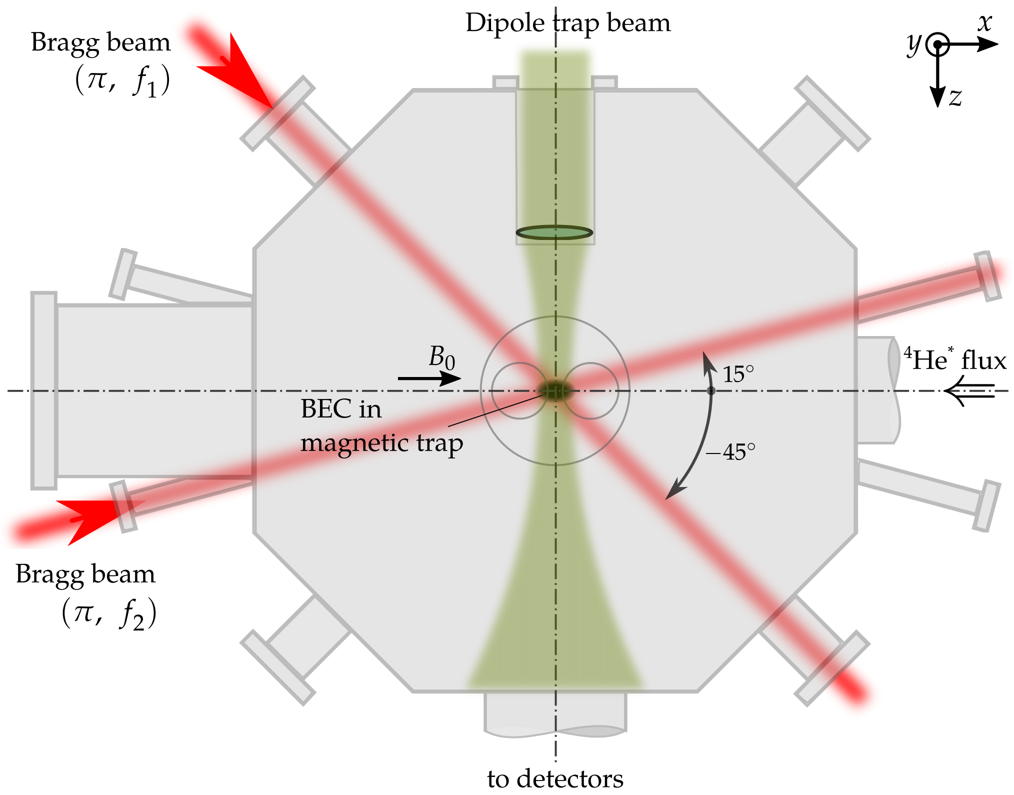

Figure 8.3: Schematic of the experimental configuration. The Bragg laser beams (red) form an angle of 60° and fully overlap with atoms in the optical dipole trap (green). This configuration results in the momentum transfer upwards under 15° with respect to the z-axis (see Fig. 8.5). The Bragg beams polarization π is in the xz-plane. Relative frequency detuning is $\Delta f = f_2 - f_1$. Also shown (not to scale): the BEC cloud and the cross-section of magnetic trap coils (BiQUIC).

confidence [7]. The atom is then released from the trap by switching off the dipole trapping beam.

8.2.2 Atom interferometer

Bragg scattering

The first step towards implementation of the interferometer is preparation and calibration of the corresponding two-photon transition. Here we employ the Bragg process due to its relative simplicity and the fact that it does not change the atomic magnetic state. The corresponding transition diagram[1] is shown in Fig. 8.4. The transitions between magnetic substates $|1,0\rangle \leftrightarrow |2,0\rangle$ and $|1,1\rangle \leftrightarrow |2,1\rangle$ can each be driven individually with the same beam setup, depending on the substate of the atoms scattered. For the initial calibration of Bragg transfer it is convenient to use atoms in the $m_J = +1$ state released from the magnetic trap. The fine-tuning of the interferometer is then performed on $m_J = 0$ atoms for the actual Wheeler experiment. Our single atom source includes the spin-flipping step via the RF transition $|1,1\rangle \rightarrow |1,0\rangle$.

For the laser beams preparation we use the same considerations and a similar optical

[1] Refer to Chapter 2 for the complete ^{4}He* levels diagram in Fig. 2.1 and the transition frequencies in Table 2.1.

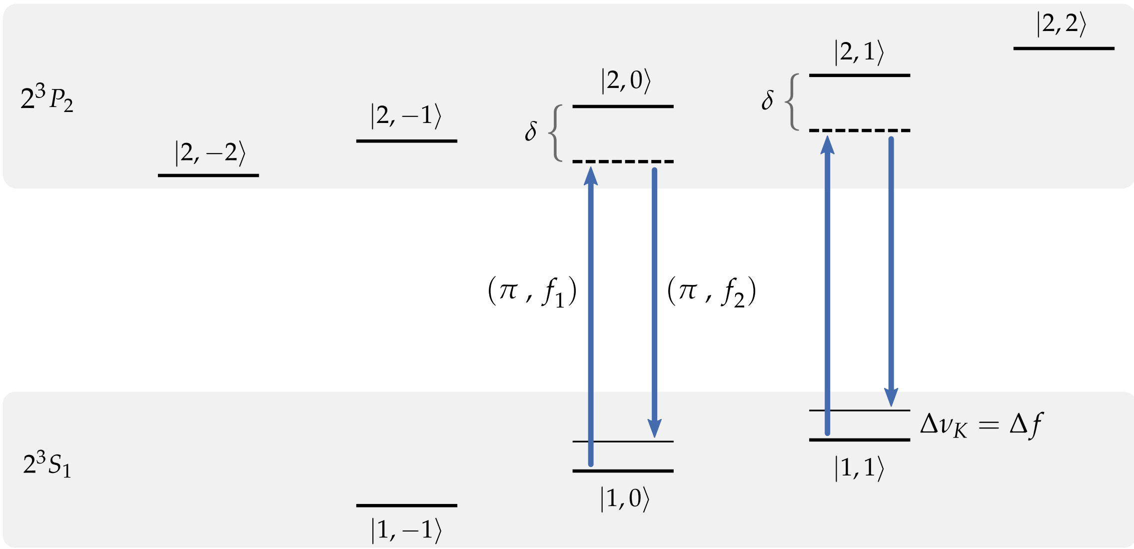

Figure 8.4: Energy level scheme for Bragg $2^3\mathrm{S}_1 - 2^3\mathrm{P}_2$ transitions. $|J, m_J\rangle$ are states of the 2^3P_2 and 2^3S_1 manifolds in $^4\mathrm{He}^*$. The atoms in $|1,+1\rangle$ are initially magnetically trapped. The arrows indicate the Bragg transitions stimulated by the laser beams with the linear polarization (π) and the relative detuning $\Delta f = f_2 - f_1$. The separation between (external) momentum states (not to scale) is $\Delta\nu_K$, corresponding to the kinetic energy $\Delta E_K = h\Delta\nu_K$ of an atom after the Bragg transition. The light frequencies $f_{1,2}$ have the detuning δ from the $2^3S_1 \to 2^3P_2$ single-photon transition occurring at the frequency ν_0. Note that $\nu_0 \gg \delta \gg \Delta\nu_K$.

layout detailed previously in a context of Bragg and Raman scattering of the BEC (see Section 5.1). The Bragg scattering laser light is provided by a 1 W ytterbium fibre laser operating at $\lambda_0 = 1083$ nm (see Fig. 5.1 for the optical layout). Here we only highlight the differences in laser pulse waveforms and beams configuration relevant to this experiment.

We use the same pulse shape modulation techniques from Section 5.1.3 and optimize the Bragg transition to occur between the two states only, resulting in the negligible transfer into higher diffraction orders (i.e. the momentum states other than the ground and first excited state). Note, that the low momentum spread for our single atom source (resulting from smaller trapping frequencies and long trap relaxation time, see Chapter 4) also improves the fidelity of Bragg scattering [158]. If, nevertheless, the atom ends up in a higher order, that particular experimental run is effectively lost[2] and does not affect the signal-to-noise ratio. This is particularly important in the Wheeler's experiment, because the high visibility in a "closed" interferometer configuration is an evidence of a wave-like behaviour.

The momenta diagram for the Bragg process is shown in Fig. 8.5. After a two-photon transition from the ground momentum state $|0\rangle$ into the first excited state $|1\rangle$ the atoms acquire velocity components along x and z axes. This makes both states easily separable in space and time as the atoms fall under gravity on the detector. The momentum transfer for the angle between the laser beams $\theta = 60°$ amounts to a single photon recoil $|\Delta\mathbf{p}^{\mathrm{He}}| = |\hbar\mathbf{k_2} - \hbar\mathbf{k_1}| = \hbar k_0$. The angle θ was chosen so that the momentum recoil was large enough to distinguish the two modes, yet not sufficient to kick the atoms beyond the detector

[2] Although the Bragg pulses are applied three times in an interferometer, the probability of multiple consecutive higher order scattering events resulting in a momentum state either $|0\rangle$ or $|1\rangle$ is negligibly small.

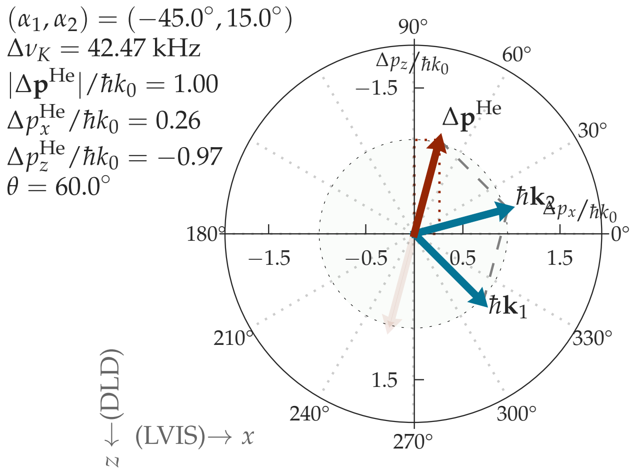

Figure 8.5: Momenta diagram for the Bragg transition. The laser beams are at the angles of −45° and 15° as in the experimental configuration in Fig. 8.3. The stimulated transition occurs by absorption of an $\hbar\mathbf{k}_2$-photon and emission of an $\hbar\mathbf{k}_1$-photon. The direction of the Bragg process is set by the sign in the detuning $\Delta f = \pm\Delta\nu_K$, which results in the two possible momentum directions: $\pm\Delta\mathbf{p}^{He}$. The relevant quantities are shown on the left (refer to Eqs. (5.2) and (5.3)). The laser beams angles α_1 and α_2 are relative to the $^4He^*$ beamline in a vacuum chamber.

radius.

As discussed previously in Section 5.1.3, the RF waveforms driving the AOMs for each of the laser beams are defined as:

$$\begin{aligned} u_1(t) &= A\, w(t) \sin(2\pi f_1 t + \phi), \\ u_2(t) &= A\, w(t) \sin(2\pi f_2 t), \end{aligned} \tag{8.1}$$

The relative phase difference between the atomic wavefunctions is introduced by setting a phase ϕ for the waveform[3] in the first beamsplitter pulse only. The relative frequency detuning is $f_2 - f_1 = \Delta f = 43$ kHz. The durations and amplitudes of the pulses were fine-tuned to minimize Fourier broadening while keeping the total length of the sequence short for the maximum interference visibility. The resulting waveforms are shown in Fig. 8.6 and the parameters are summarized in Table 8.1. The total duration of the interferometer sequence is 250 µs and it is sampled into 500,000 time data points for the arbitrary waveform generator. The interferometer uses a $\pi/2 - \pi - \pi/2$ pulse sequence (Fig. 8.6).

Random delayed choice. To provide the "delayed choice" for the experiment, the RF switch randomly enables/disables the Bragg AOMs to determine whether the second beamsplitting pulse is applied 70 µs after the mirror pulse finishes. We implement this using the so called output bit from a quantum random bit generator (QRNG) which is latched 170 µs after the interferometer pulse sequence starts. This bit is then sets a TTL control signal for the Bragg AOMs electronics.

The quantum random number generation is one of the most mature quantum technologies, as the inherent randomness at the core of quantum mechanics makes quantum

[3]The arbitrary waveform generator Agilent 81150A has a phase locked dual channel output with measured temporal jitter between the channels ∼1 ns.

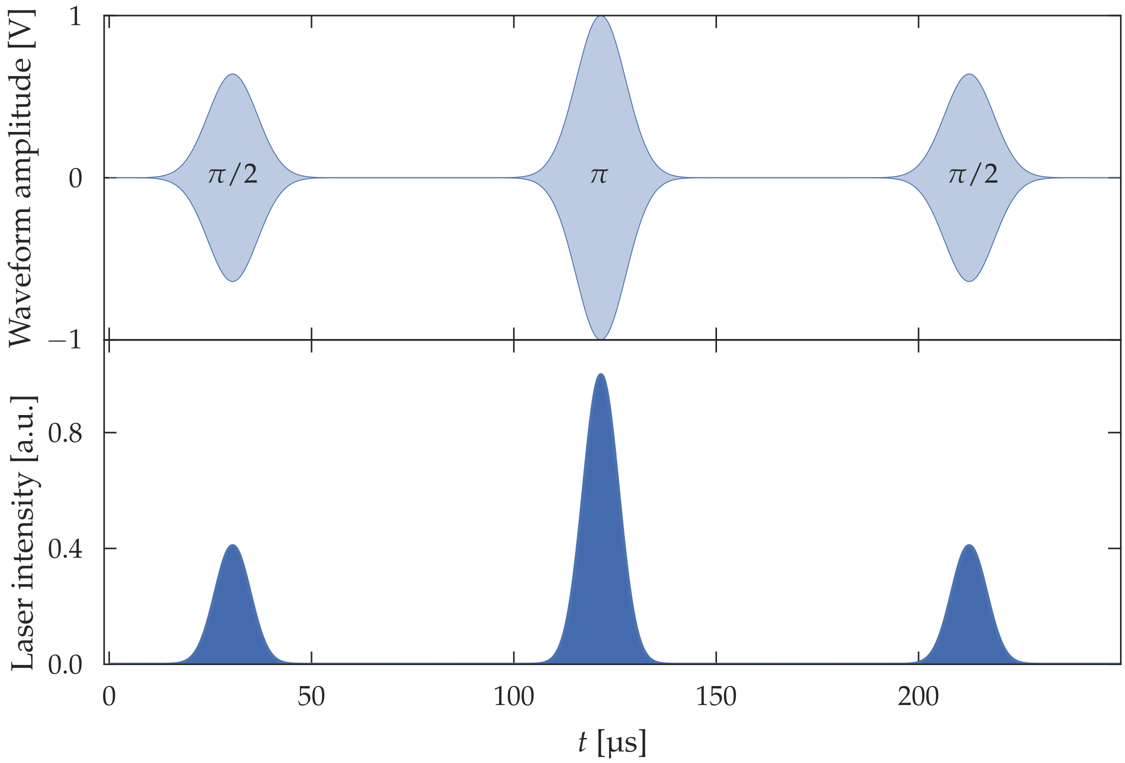

Figure 8.6: Temporal envelope of the interferometer pulse sequence. Analog waveforms $u_{1,2}(t)$ (top) and the resulting pulse intensity $|u_{1,2}(t)|^2$ (bottom). The waveforms were uploaded into the arbitrary waveform generator to drive acousto-optic modulators. The Fourier broadening of each pulse was optimised to minimize the transfer to the higher Bragg diffraction orders. The amount of a corresponding Rabi oscillation introduced by each pulse is indicated by $\pi/2$ for the"beamsplitter" pulses and by π for the "mirror" pulse.

systems a perfect source of entropy [159]. In out experiments we use a commercially available unit[4] implementing a branching path optical binary QRNG. It utilizes a randomness in the transmission/reflection of the photon from an LED impinging onto a balanced 50/50 beam splitter. The photon is subsequently detected by a single-photon detector. Note, that for our purposes, the exact probability of getting 0 or 1 as an output bit is not crucial (although this probability is close to 0.50), what is important is the *true* randomness which is guaranteed by the unit's design [159, 160].

Pulse	Operation	Pulse duration	A	α
$\pi/2$	beamsplitter	$t^{(\pi/2)} = 61$ μs	0.64	5
π	mirror	$t^{(\pi)} = 61$ μs	1.00	5

Table 8.1: Waveform parameters of the interferometer pulse sequences. The pulse duration gives the length of a Gaussian modulated pulse, with (π) and $(\pi/2)$ indicating the amount of a corresponding Rabi oscillation. The modulation depth α and the amplitude A are as in Eqs. (5.6)-(5.8). The waveforms are plotted in Fig. 8.6.

[4]Quantis OEM quantum random bit generator (ID Quantique, model number: Quantis, P/N:0600684A210), Patent US 7519641 B2 [160].

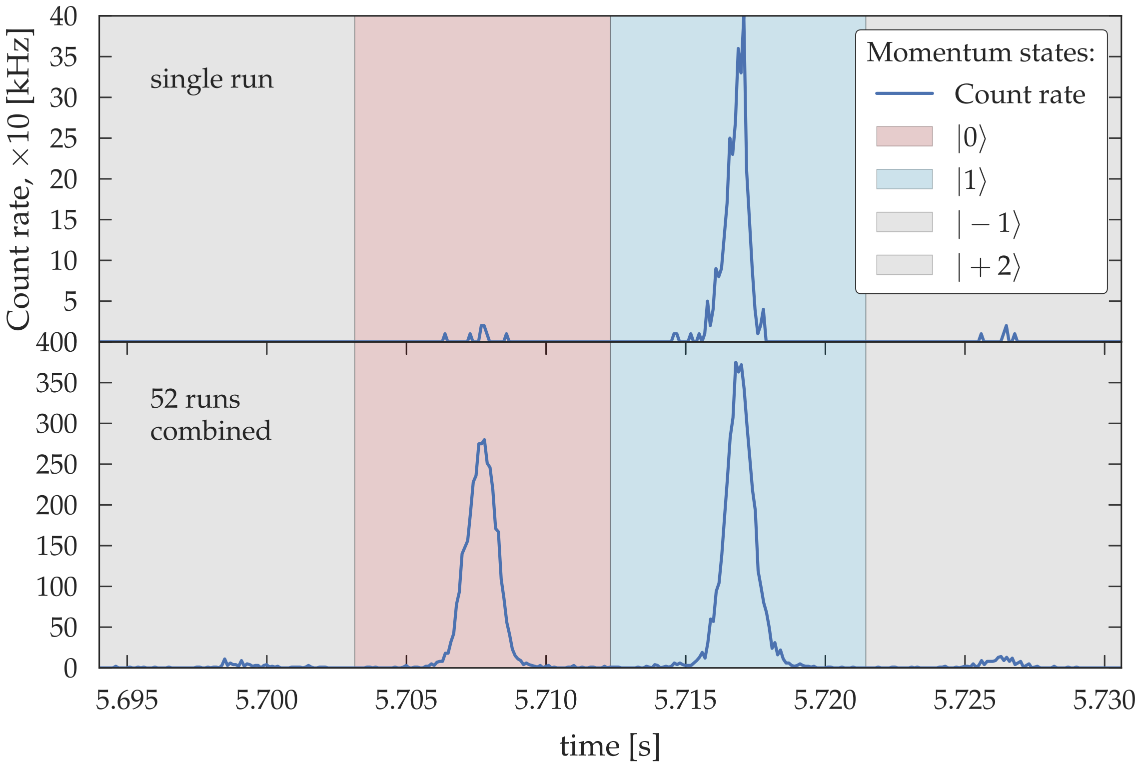

Figure 8.7: Bragg transfer: time-of-flight measurement. A single experimental run for the Bragg transfer (top) and the combined 52 runs (bottom) for the two full Rabi oscillation cycles (shown in Fig. 8.8). Highlighted are the output ports for each of the corresponding momentum states. The atoms reaching $|1\rangle$ port arrive at a slightly latter time than those in $|0\rangle$ port due to the received upwards component of the momentum kick. The data for a single run shows a maximum Bragg transfer, i.e. a π-pulse condition.

Rabi oscillation of the Bragg transfer. Before constructing a full interferometer sequence, the performance of the scattering process was first characterised with a single Bragg pulse. For that we use the clouds containing a large number of atoms in the $m_J = 1$ magnetic substate, in the same optical dipole trap that will eventually be used for the single $m_J = 0$ atom when performing Wheeler's experiment. The Bragg beams, each having $\sim$155 mW of power, are applied $\sim$1 ms after the atoms are released from the dipole trap and have a detuning $\delta \approx 280$ GHz to the red of the $2^1S_0 - 2^3P_2$ transition, and a relative detuning of $\Delta f = 47$ kHz between the beams. The two-photon detuning δ was chosen to be at least a few hundreds of GHz to reduce the sensitivity to long-term drifts in the laser frequency, in addition to reducing the spontaneous scattering rate. Diameter of each Bragg beam at the position of the optical trap is 5–6 mm.

The time-of-flight measurement of the population transfer with MCP/DLD is illustrated in Fig. 8.7. The top plot for a single experimental run (representing a "mirror" operation) corresponds to the single data point in Fig. 8.8 which demonstrates two full Rabi cycles – the relative populations oscillate between momentum modes as a function of the laser pulse duration. All the other waveform parameters are kept constant. Here, and for the other Bragg transfer tests, only the first pulse from the $(\pi/2 - \pi - \pi/2)$ sequence is used (Fig. 8.6). The portion of the cloud occupying two modes was determined from counting the number of atoms measured in the two physically separated ports as illustrated in Fig. 8.7. The maximum transfer into $|1\rangle$ mode occurs when the laser power

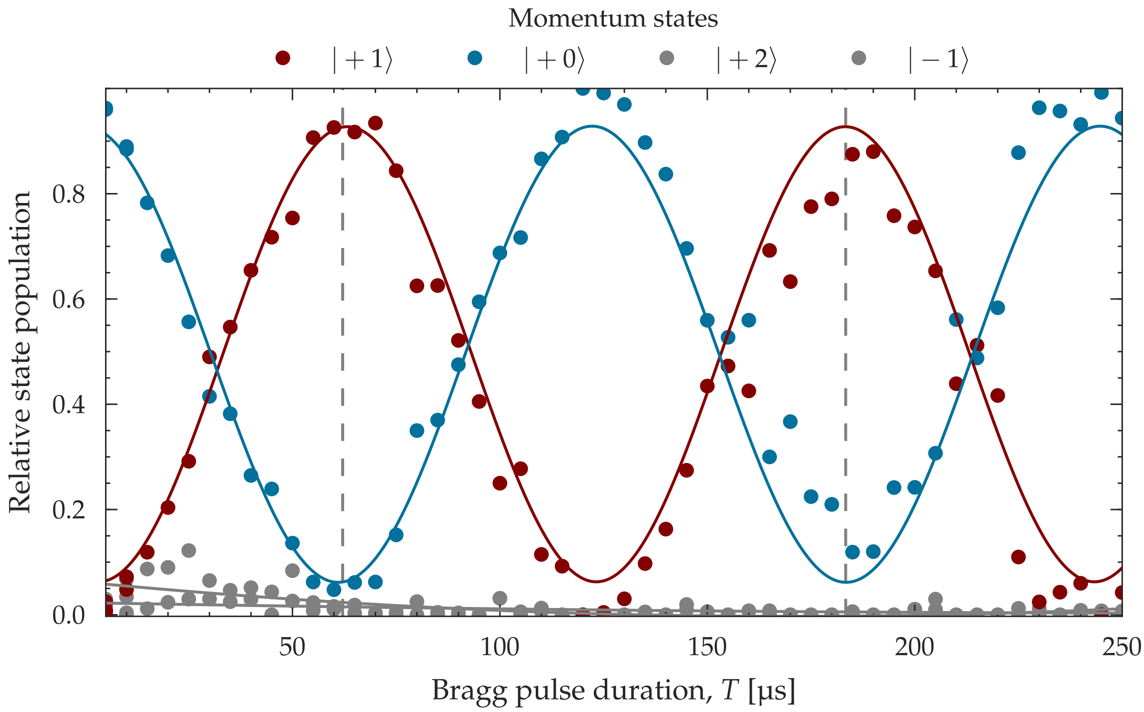

Figure 8.8: Bragg transfer. States populations for the two-level Rabi oscillation between the $|0\rangle$ (trapped BEC) and $|+1\rangle$ momentum states. Atoms are transferred by the laser Bragg pulses with varied duration for each data point. The population fraction is relative to the initial number of trapped atoms. Maximum transfer into the $|+1\rangle$ state occurs for laser power corresponding to the π- and 3π-pulse conditions (vertical dashed lines). The population curves are fitted with the expected sine shapes. A small fraction of the atoms transferred into $|-1\rangle$ and $|+2\rangle$ states is shown in grey.

corresponds to the Bragg π-pulse. However, because of the detector saturation effects, it is practical to fine-tune the parameters of a π-pulse by minimizing the leftover in the $|0\rangle$ mode. A sinusoidal oscillation of the mode occupations is clearly seen as the duration of the Bragg pulse changes, which fits to a transfer efficiency of $\approx$ 96%.

Interferometer calibration. The complete Mach-Zehnder interferometer can then be realised by applying the full sequence of three Bragg pulses to the atoms. After testing with large numbers of $m_J = +1$ atoms we proceed to refining the interferometer parameters using $m_J = 0$ atoms, thus compensating for possible differences in Rabi frequency for two magnetic substates. Those differences may be related to the magnetic field gradients which shift the position of atoms in an optical trap and therefore result in a slightly changed overlap with the Bragg beams. Also, after the magnetically sensitive atoms are released from the trap, their path is slightly deflected by the magnetic fields before the Bragg beams are applied (1 ms after the trap switch-off).

The performance of the interferometer is illustrated by Fig. 8.9, which shows the data from MCP/DLD using relatively large number of $\sim$8000 atoms in $m_J = 0$ substate. The outputs of $|0\rangle$ and $|1\rangle$ ports oscillate in accordance with a phase difference between atomic wavefunctions introduced by the beamsplitter pulse, thus clearly demonstrating an interference. Its visibility is shown in Fig. 8.10, the mode populations are calculated in the same way as the Rabi cycle results above.

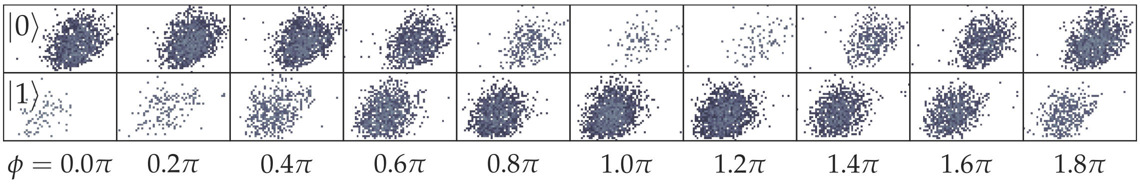

Figure 8.9: Ramsey fringes for the Mach-Zehnder interferometer. Spatial images of the output ports of the interferometer in the MCP/DLD plane are formed by histogramming counts which are time-windowed at the ports $|0\rangle$ (top row), and $|1\rangle$ (bottom row) as in Fig. 8.7. Populations oscillate between the momentum modes as a function of the interferometer phase. Each phase value represents a single experimental run (no averages).

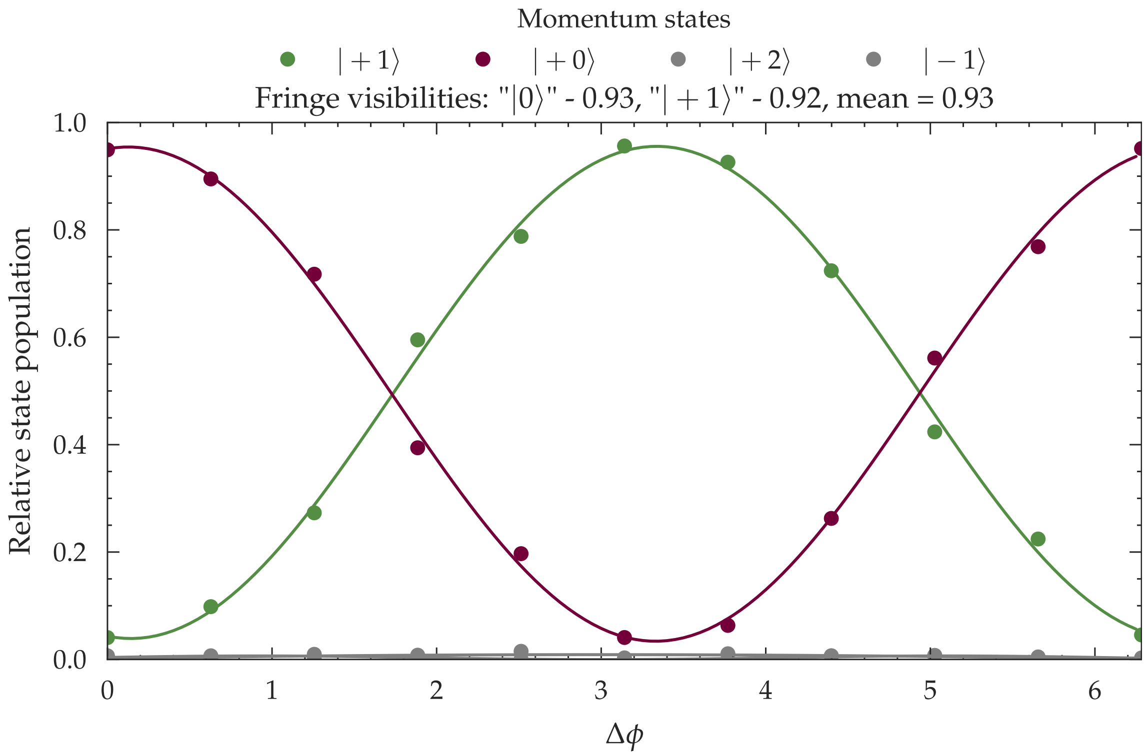

Figure 8.10: Interference visibility. State populations for the Ramsey fringe shown in Fig. 8.9. The green data represents the counts observed at the $|0\rangle$ output port, while the red data represents the $|1\rangle$ port. The average fringe visibility is 92%. Each phase value represents a single experimental run (no averages). The population curves are fitted with the expected sine shapes.

8.3 Results and discussion

8.3.1 Interference visibility

The atoms are measured on the DLD as before, however the configuration of the interferometer is also recorded by the delay-line electronics so that the result of the random choice for each experimental iteration can be recovered. The TTL signal from the digital latch is sent to a pulse generator, where a high level results in a sequence of NIM pulses being registered on a channel of the time to digital converter not used for the delay-line wires, while a low level does not generate such pulses. Thus, during the data analysis process undertaken using the files written to our data acquisition workstation, the pres-

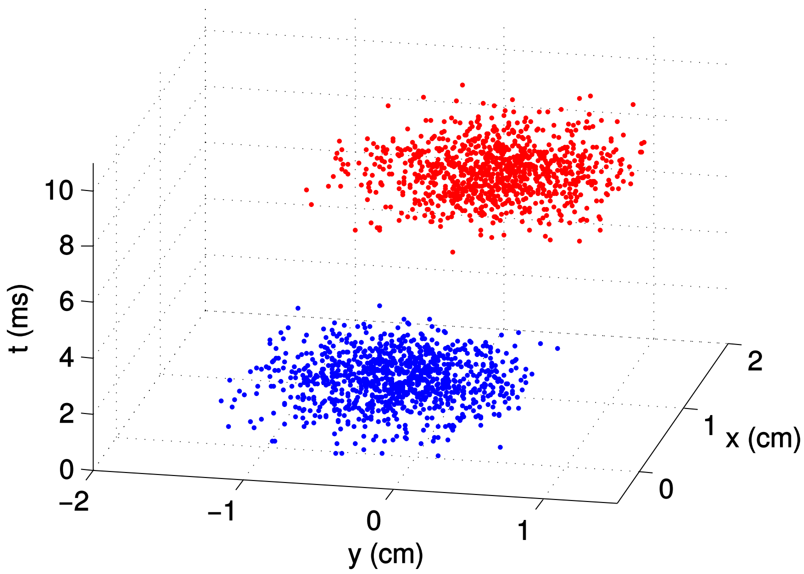

Figure 8.11: Output ports of the interferometer. Spatial and temporal locations of the output ports of the interferometer, showing the well resolved detection locations. The blue data represents the counts observed at the $|0\rangle$ output port, while the red data represents the $|1\rangle$ port. The atoms reaching $|1\rangle$ port arrive at a slightly latter time than those in $|0\rangle$ port due to the upwards component of the momentum kick they receive from the Bragg pulses.

ence of these pulses identifies the interferometer configuration for each shot.

As the data acquisition rates for a single atom source are low (see methods), we first demonstrate a delayed choice interferometer with $\sim$1000 atoms per experimental cycle in the inset of Fig. 8.12, where the result for each choice of ϕ is the average of 20 experimental cycles. The distinction between the removal (red points) and application (blue points) of the mixing $\pi/2$-pulse is very clear, as the former is $\sim$50% irrespective of the phase ϕ, while the latter shows the expected sinusoidal dependence on ϕ typical of a Mach-Zehnder interferometer.

8.3.2 Main result: single atom delayed choice experiment

This experimental procedure is then reproduced with a true single atom source (see Ch. 4 and Ref. [7]), and compared to the large number result. The result of this is shown in Fig. 8.12, where each experimental point is now the average of several thousand experimental cycles. It can be seen that the experimental points closely resemble that of Fig. 8.12 (inset), where fits to the experimental data give similar results to the large number case. The main additional source of error for this data compared to the large number version is shot noise due to limited counts. Also, the single atom data is more susceptible to long term drifts in the experiment as data acquisition takes several weeks, as opposed to several hours for the large number result.

As in the optical case [82] we require each detector (see Figs. 8.2, 8.11) to be unambiguously correlated to the path the atom took through the interferometer. To test this assumption, we use the "which-way" parameter $I = (N_1 - N_2)/(N_1 + N_2)$ where N_1 and N_2 are the number of atoms measured at the output ports with the interferometer in the "open" configuration [147, 161, 162]. We measure $I = 0.97(\pm 0.05)$ when the first

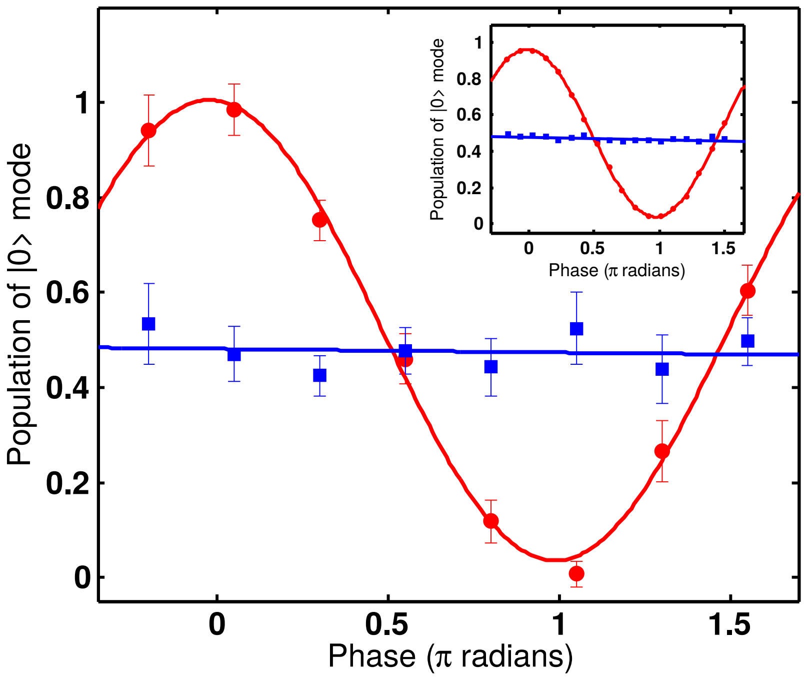

Figure 8.12: Wheeler's delayed choice experiment with massive bodies. Here the population of $|0\rangle$ mode is a normalised probability of finding atoms in the $m_J = 0$ state. Blue squares represent the "open" configuration and red dots represent the "closed" configuration of the interferometer. The inset shows the result when a large number of atoms ~1000 are used, in such case the error bars (1 standard deviation) are smaller than the data symbols used. The main result shown in the central figure is produced using a single atom, with each point being the cumulative result of a few thousand runs of the experiment and the error bars representing the statistical spread of the data. The solid lines are fits to the data, with the closed configuration fitting well to a sinusoidal form with a visibility of 0.98 ± 0.05. A linear fit to the open configuration has a slight slope due to imperfections in our Bragg pulses.

beamsplitting pulse is absent – effectively allowing only one path through the interferometer. To check the other path we replace the first beamsplitting pulse with a mirror pulse, here we measure $I = 0.95(\pm 0.05)$, indicating that the ports of the interferometer allow excellent which-way information.

Further to this analysis, we can estimate the visibility when the interferometer is in the "open" configuration by fitting a sinusoidal curve to the "open" data (blue squares in Fig. 8.11) and find a value of $V = 0.03(\pm 0.04)$. Consistent with theoretical predictions [147, 163] and demonstrated for the more general intermediate case with photons [164] we expect the complementarity parameter for our interferometer to follow the inequality: $V^2 + D^2 \leq 1$. For the "open" case we measure $V^2 + D^2 = 0.92(\pm 0.08)$, where D is the distinguishability, given by the average of the which-way parameters. In the absence of information loss, one expects the complementarity parameter to be unity, in our case, the deviation from unity is attributable to imperfections in the Bragg pulses which reduce our distinguishability. The "closed" configuration could be investigated in an analogous way by implementing the final beamsplitter, as could the intermediate case in which the Bragg beamsplitter pulse reflectivity is varied.

Simple "which way" test. To illustrate this, for example, Fig. 8.13 shows the very simple "which-way" ("Welcher Weg") test without the last beamspitter. The reflectivity of the first beamsplitter was set from 50% to nearly 100% by replacing it with the "mirror" pulse, effectively modifying the first two pulses from the standard interferometer pulse sequence to: $(\pi - \pi)$. As expected, the output of the modified in this way "open" interferometer switched from deterministic to random as the reflectivity of the first beamsplitter was switched from 100% back to 50%. The first case in Fig. 8.13 corresponds to the trivial case when the middle π-pulse only is present from the sequence, and the last is simply two π-pulses resulting in the net 2π Rabi oscillation.

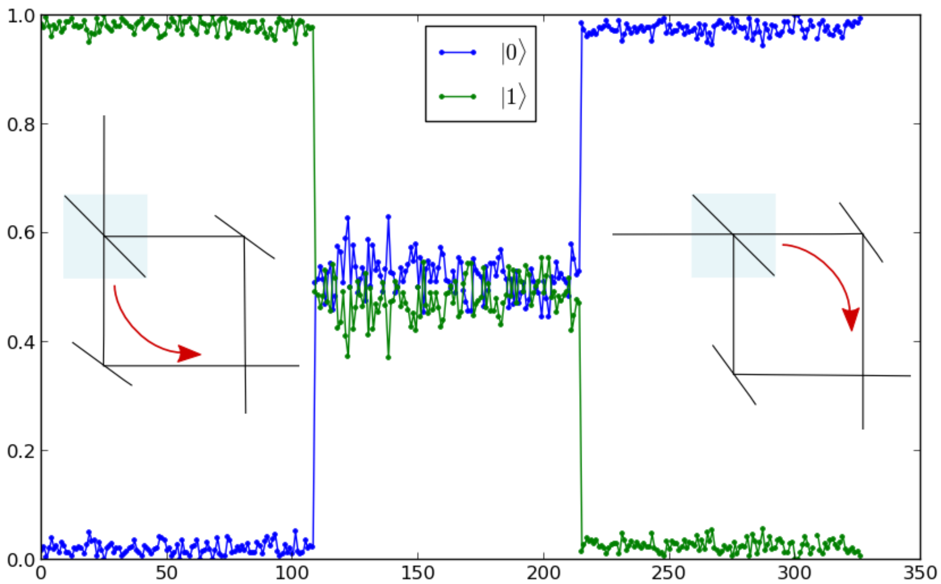

Figure 8.13: Which-way demonstration. The output of the "open" interferometer shows population fraction in each of the momentum modes $|0\rangle$ (blue data points) and $|1\rangle$ (green). In the free-run mode of the experiment, the Bragg pulse sequence was changed from $(-\pi-)$ to $(\pi/2 - \pi-)$ and then to $(\pi - \pi-)$, which corresponds to the first beamsplitter reflectivities: 0%, 50%, 100%. The which-way information is lost only for the case of first beamsplitter having 50% reflectivity. Every data point represents a single experimental run.

We can quantify the single atom nature of our source by analyzing the statistics of atoms arriving at the output ports of the interferometer. To this end we calculate the second order correlation function for the data shown in Fig. 8.14. We measure, see Fig. 8.14, a correlation function indicative of a strongly sub-poissonian source, with a correlation parameter α [67] (equivalent to $g^{(2)}(0)$) of $\alpha = 0.07(\pm 0.03)$. The deviation we observe away from a perfect single atom source ($\alpha = 0$) is readily explained via the measured dark count rate of our detector, with the probability of observing a real count and a dark count in the same run of the experiment, yielding a lower limit to α of 0.06. This equates to observing, out of the nearly 30,000 runs of the experiment, ten runs in which two counts are observed.

It is interesting to contrast the photon demonstration of Wheeler's experiment [82] with the atomic one performed here. In the photon case the timing of the experiment is

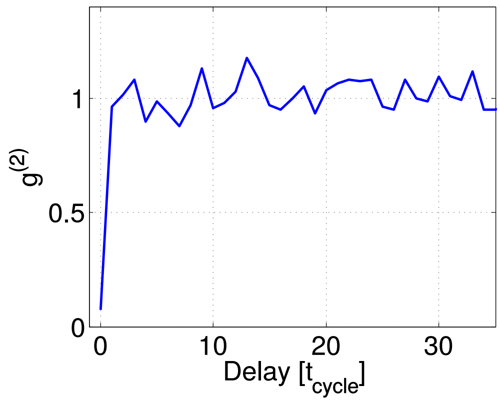

Figure 8.14: Second order correlation function of atoms arriving at the output ports of our interferometer as a function of the delay between experimental runs. Here the delay is in units of the cycle time of the experiment, $t_{\text{cycle}} = 35$ s.

such that the small temporal width of the single photon source (45 ns), combined with a large interferometer size (48 m), allow the choice event to be space-like separated from the event where the photon reaches the first beamsplitter. In our experiment, the first beamsplitter is a light pulse which spatially overlaps the single atom source, and thus the relevant temporal width for this operation is simply the duration of the $\pi/2$ pulse. Thus space-like separation in our experiment is unfeasible, however, the slow velocity of the atom does allow a delayed choice in time, as implemented here.

In conclusion, this proposed method strives towards the goal of observing exciting new phenomena with massive particles, and shows that the capabilities of experiments in quantum atom optics are quickly catching up to their photonic counterparts.

References

[1] S. S. Hodgman, R. I. Khakimov, R. J. Lewis-Swan, A. G. Truscott, and K. V. Kheruntsyan. "Solving the Quantum Many-Body Problem via Correlations Measured with a Momentum Microscope". **Phys. Rev. Lett. 118** (2017), 240402. DOI: 10.1103/PhysRevLett.118.240402 (cited on p. 17).

[2] R. I. Khakimov, B. M. Henson, D. K. Shin, S. S. Hodgman, R. G. Dall, K. G. H. Baldwin, and A. G. Truscott. "Ghost imaging with atoms". **Nature 540** (2016), 100–103. DOI: 10.1038/nature20154 (cited on pp. 17, 44).

[3] D. K. Shin, B. M. Henson, R. I. Khakimov, J. A. Ross, C. J. Dedman, S. S. Hodgman, K. G. H. Baldwin, and A. G. Truscott. "Widely tunable, narrow linewidth external-cavity gain chip laser for spectroscopy between 1.0 – 1.1 µm". **Opt. Express 24** (2016), 27403–27414. DOI: 10.1364/OE.24.027403.

[4] A. G. Manning, R. I. Khakimov, R. G. Dall, and A. G. Truscott. "Wheeler's delayed-choice gedanken experiment with a single atom". **Nature Physics 11** (2015), 539. DOI: 10.1038/nphys3343 (cited on pp. 11, 47, 59).

[5] B. M. Henson, R. I. Khakimov, R. G. Dall, K. G. H. Baldwin, L.-Y. Tang, and A. G. Truscott. "Precision Measurement for Metastable Helium Atoms of the 413 nm Tune-Out Wavelength at Which the Atomic Polarizability Vanishes". **Phys. Rev. Lett. 115** (2015), 043004. DOI: 10.1103/PhysRevLett.115.043004 (cited on p. 74).

[6] C. J. Dedman, B. M. Henson, R. I. Khakimov, A. G. Truscott, and R. G. Dall. "Precision temperature controlled filtered laminar air enclosure". **Measurement Science and Technology 26** (2015), 027002. DOI: 10.1088/0957-0233/26/2/027002.

[7] A. G. Manning, R. I. Khakimov, R. G. Dall, and A. G. Truscott. "Single-Atom Source in the Picokelvin Regime". **Phys. Rev. Lett. 113** (2014), 130403. DOI: 10.1103/PhysRevLett.113.130403 (cited on pp. 11, 12, 60, 62, 63, 70).

[8] C. Adams, M. Sigel, and J. Mlynek. "Atom optics". *Physics Reports* 240 (1994), 143–210. DOI: 10.1016/0370-1573(94)90066-3 (cited on p. 2).

[9] G. Drake. *Springer Handbook of Atomic, Molecular, and Optical Physics*. Springer Handbook of Atomic, Molecular, and Optical Physics. Springer, 2006 (cited on pp. 4, 39).

[10] A. D. Cronin, J. Schmiedmayer, and D. E. Pritchard. "Optics and interferometry with atoms and molecules". *Rev. Mod. Phys.* 81 (2009), 1051–1129. DOI: 10.1103/RevModPhys.81.1051 (cited on pp. 4, 60).

[11] A. Kramida, Yu. Ralchenko, J. Reader, and NIST ASD Team. NIST Handbook of Basic Atomic Spectroscopic Data, National Institute of Standards and Technology, Gaithersburg, MD. 2015 (cited on p. 4).

[12] A. Kramida, Yu. Ralchenko, J. Reader, and NIST ASD Team. NIST Atomic Spectra Database (v5.3), National Institute of Standards and Technology, Gaithersburg, MD. 2015 (cited on pp. 4, 5).

[13] S. Gupta, A. E. Leanhardt, A. D. Cronin, and D. E. Pritchard. "Coherent manipulation of atoms with standing light waves". *Comptes Rendus de l'Académie des Sciences - Series IV - Physics* 2 (2001), 479–495. DOI: 10.1016/S1296-2147(01)01179-9 (cited on p. 4).

[14] M. Kozuma, L. Deng, E. W. Hagley, J. Wen, R. Lutwak, K. Helmerson, S. L. Rolston, and W. D. Phillips. "Coherent Splitting of Bose-Einstein Condensed Atoms with Optically Induced Bragg Diffraction". *Phys. Rev. Lett.* 82 (1999), 871–875. DOI: 10.1103/PhysRevLett.82.871 (cited on p. 5).

[15] K. Bongs and K. Sengstock. "Physics with coherent matter waves". *Reports on Progress in Physics* 67 (2004), 907 (cited on p. 5).

[16] T. Kovachy, S.-w. Chiow, and M. A. Kasevich. "Adiabatic-rapid-passage multiphoton Bragg atom optics". *Phys. Rev. A* 86 (2012), 011606. DOI: 10.1103/PhysRevA.86.011606 (cited on p. 5).

[17] W. Vassen, R. P. M. J. W. Notermans, R. J. Rengelink, and R. F. H. J. van der Beek. "Ultracold metastable helium: Ramsey fringes and atom interferometry". *Applied Physics B* 122 (2016), 289. DOI: 10.1007/s00340-016-6563-0 (cited on pp. 5, 6).

[18] H. Müller, S.-w. Chiow, and S. Chu. "Atom-wave diffraction between the Raman-Nath and the Bragg regime: Effective Rabi frequency, losses, and phase shifts". *Phys. Rev. A* 77 (2008), 023609. DOI: 10.1103/PhysRevA.77.023609 (cited on p. 5).

[19] D. E. Pritchard and P. L. Gould. "Experimental possibilities for observation of unidirectional momentum transfer to atoms from standing-wave light". *J. Opt. Soc. Am. B* 2 (1985), 1799–1804. DOI: 10.1364/JOSAB.2.001799 (cited on p. 5).

[20] P. J. Martin, B. G. Oldaker, A. H. Miklich, and D. E. Pritchard. "Bragg scattering of atoms from a standing light wave". *Phys. Rev. Lett.* 60 (1988), 515–518. DOI: 10.1103/PhysRevLett.60.515 (cited on pp. 5, 60).

[21] H. Batelaan. "The Kapitza-Dirac effect". *Contemporary Physics* 41 (2000), 369–381. DOI: 10.1080/001075100100001220 (cited on p. 5).

[22] D. L. Freimund and H. Batelaan. "Bragg Scattering of Free Electrons Using the Kapitza-Dirac Effect". *Phys. Rev. Lett.* 89 (2002), 283602. DOI: 10.1103/PhysRevLett.89.283602 (cited on p. 5).

[23] Freimund Daniel L., Aflatooni Kayvan, and Batelaan Herman. "Observation of the Kapitza-Dirac effect". *Nature* 413 (2001). 10.1038/35093065, 142–143. DOI: http://dx.doi.org/10.1038/35093065 (cited on p. 5).

[24] H. Batelaan. "*Colloquium* : Illuminating the Kapitza-Dirac effect with electron matter optics". *Rev. Mod. Phys.* 79 (2007), 929–941. DOI: 10.1103/RevModPhys.79.929 (cited on p. 5).

[25] L Gould, G. a. Ruff, and David E. Pritchard. "Diffraction of Atoms by Light: The Near-Resonant Kapitza-Dirac Effect". *Physical Review Letters* 56 (1986) (cited on pp. 5, 6, 44, 46).

[26] P. J. Martin, P. L. Gould, B. G. Oldaker, A. H. Miklich, and D. E. Pritchard. "Diffraction of atoms moving through a standing light wave". *Phys. Rev. A* 36 (1987), 2495–2498. DOI: 10.1103/PhysRevA.36.2495 (cited on p. 5).

[27] P. Sancho. "Two-particle Kapitza-Dirac diffraction". *Phys. Rev. A* 82 (2010), 033814. DOI: 10.1103/PhysRevA.82.033814 (cited on p. 5).

[28] P. Sancho. "The Bragg regime of the two-particle Kapitza–Dirac effect". *Journal of Physics B: Atomic, Molecular and Optical Physics* 44 (2011), 145002 (cited on p. 5).

[29] X. Li, J. Zhang, Z. Xu, P. Fu, D.-S. Guo, and R. R. Freeman. "Theory of the Kapitza-Dirac Diffraction Effect". *Phys. Rev. Lett.* 92 (2004), 233603. DOI: 10.1103/PhysRevLett.92.233603 (cited on p. 5).

[30] L. Rosenberg. "Extended theory of Kapitza-Dirac scattering". *Phys. Rev. A* 70 (2004), 023401. DOI: 10.1103/PhysRevA.70.023401 (cited on p. 5).

[31] Y. B. Ovchinnikov, J. H. Müller, M. R. Doery, E. J. D. Vredenbregt, K. Helmerson, S. L. Rolston, and W. D. Phillips. "Diffraction of a Released Bose-Einstein Condensate by a Pulsed Standing Light Wave". *Phys. Rev. Lett.* 83 (1999), 284–287. DOI: 10.1103/PhysRevLett.83.284 (cited on pp. 5, 44, 46).

[32] B. Gadway, D. Pertot, R. Reimann, M. G. Cohen, and D. Schneble. "Analysis of Kapitza-Dirac diffraction patterns beyond the Raman-Nath regime". *Opt. Express* 17 (2009), 19173–19180. DOI: 10.1364/OE.17.019173 (cited on p. 5).

[33] B. R. Gadway. *Bose Gases in Tailored Optical and Atomic Lattices*. STATE UNIVERSITY OF NEW YORK AT STONY BROOK, 2012 (cited on p. 5).

[34] S. Eilzer, H. Zimmermann, and U. Eichmann. "Strong-Field Kapitza-Dirac Scattering of Neutral Atoms". *Phys. Rev. Lett.* 112 (2014), 113001. DOI: 10.1103/PhysRevLett.112.113001 (cited on p. 5).

[35] O. Smirnova, D. L. Freimund, H. Batelaan, and M. Ivanov. "Kapitza-Dirac Diffraction without Standing Waves: Diffraction without a Grating?" *Phys. Rev. Lett.* 92 (2004), 223601. DOI: 10.1103/PhysRevLett.92.223601 (cited on p. 6).

[36] Gerlich Stefan, Hackermuller Lucia, Hornberger Klaus, Stibor Alexander, Ulbricht Hendrik, Gring Michael, Goldfarb Fabienne, Savas Tim, Muri Marcel, Mayor Marcel, and Arndt Markus. "A Kapitza-Dirac-Talbot-Lau interferometer for highly polarizable molecules". *Nat Phys* 3 (2007). 10.1038/nphys701, 711–715. DOI: http://dx.doi.org/10.1038/nphys701 (cited on p. 6).

[37] S. McGregor, W. C.-W. Huang, B. A. Shadwick, and H. Batelaan. "Spin-dependent two-color Kapitza-Dirac effects". *Phys. Rev. A* 92 (2015), 023834. DOI: 10.1103/PhysRevA.92.023834 (cited on p. 6).

[38] P. Sancho. "Diffraction of entangled particles by light gratings". *Annals of Physics* 355 (2015), 143–152. DOI: 10.1016/j.aop.2015.02.010 (cited on p. 6).

[39] A. G. Hayrapetyan, K. K. Grigoryan, J. B. Götte, and R. G. Petrosyan. "Kapitza–Dirac effect with traveling waves". *New Journal of Physics* 17 (2015), 082002 (cited on p. 6).

[40] M. M. Dellweg and C. Müller. "Influence of laser pulse shape and spectral composition on strong-field Kapitza-Dirac scattering". *Journal of Physics: Conference Series* 594 (2015), 012015 (cited on p. 6).

[41] M. A. Kasevich. "Atom interferometry with Bose–Einstein condensed atoms". *Comptes Rendus de l'Académie des Sciences - Series IV - Physics* 2 (2001), 497–507. DOI: 10.1016/S1296-2147(01)01181-7 (cited on p. 6).

[42] A Miffre, M Jacquey, M Büchner, G Trénec, and J Vigué. "Atom interferometry". *Physica Scripta* 74 (2006), C15 (cited on p. 6).

[43] O. Carnal and J. Mlynek. "Young's double-slit experiment with atoms: A simple atom interferometer". *Physical review letters* 66 (1991), 2689 (cited on p. 6).

[44] C. Bordé. "Atomic interferometry with internal state labelling". *Physics Letters A* 140 (1989), 10–12. DOI: 10.1016/0375-9601(89)90537-9 (cited on p. 6).

[45] D. W. Keith, C. R. Ekstrom, Q. A. Turchette, and D. E. Pritchard. "An interferometer for atoms". *Phys. Rev. Lett.* 66 (1991), 2693–2696. DOI: 10.1103/PhysRevLett.66.2693 (cited on p. 6).

[46] M. Kasevich and S. Chu. "Atomic interferometry using stimulated Raman transitions". *Physical review letters* 67 (1991), 181 (cited on p. 6).

[47] M. Kasevich and S. Chu. "Measurement of the gravitational acceleration of an atom with a light-pulse atom interferometer". *Applied Physics B* 54 (1992), 321–332. DOI: 10.1007/BF00325375 (cited on p. 6).

[48] Rosi G., D'Amico G., Cacciapuoti L., Sorrentino F., Prevedelli M., Zych M., Brukner Č., and Tino G. M. "Quantum test of the equivalence principle for atoms in coherent superposition of internal energy states". *Nature Communications* 8 (2017), 15529. DOI: http://dx.doi.org/10.1038/ncomms1552910.1038/ncomms15529 (cited on p. 6).

[49] Bucker Robert, Grond Julian, Manz Stephanie, Berrada Tarik, Betz Thomas, Koller Christian, Hohenester Ulrich, Schumm Thorsten, Perrin Aurelien, and Schmiedmayer Jorg. "Twin-atom beams". *Nat Phys* 7 (2011). 10.1038/nphys1992, 608–611. DOI: http://dx.doi.org/10.1038/nphys1992 (cited on p. 6).

[50] M. Bonneau, J. Ruaudel, R. Lopes, J. C. Jaskula, a. Aspect, D. Boiron, and C. I. Westbrook. "Tunable source of correlated atom beams". *Physical Review A - Atomic, Molecular, and Optical Physics* 87 (2013), 1–5. DOI: 10.1103/PhysRevA.87.061603 (cited on p. 7).

[51] K. M. Hilligsøe and K. Mølmer. "Phase-matched four wave mixing and quantum beam splitting of matter waves in a periodic potential". *Phys. Rev. A* 71 (2005), 041602. DOI: 10.1103/PhysRevA.71.041602 (cited on p. 7).

[52] G. K. Campbell, J. Mun, M. Boyd, E. W. Streed, W. Ketterle, and D. E. Pritchard. "Parametric Amplification of Scattered Atom Pairs". *Phys. Rev. Lett.* 96 (2006), 020406. DOI: 10.1103/PhysRevLett.96.020406 (cited on p. 7).

[53] A. Perrin, H. Chang, V. Krachmalnicoff, M. Schellekens, D. Boiron, A. Aspect, and C. I. Westbrook. "Observation of Atom Pairs in Spontaneous Four-Wave Mixing of Two Colliding Bose-Einstein Condensates". *Phys. Rev. Lett.* 99 (2007), 150405. DOI: 10.1103/PhysRevLett.99.150405 (cited on pp. 7, 16, 17, 37, 38, 44, 46, 48, 49, 53, 54).

[54] R. Lopes. "An atomic Hong-Ou-Mandel experiment". PhD thesis. 2015 (cited on p. 7).

[55] A. Imanaliev. "Towards testing Bell's inequality using atoms correlated in momentum". Theses. Université Paris-Saclay, 2016 (cited on p. 7).

[56] R Thomas, K. Roberts, E Tiesinga, A. Wade, P. Blakie, A. Deb, and N Kjærgaard. "Multiple scattering dynamics of fermions at an isolated p-wave resonance". *Nature Communications* 7 (2016) (cited on p. 7).

[57] R. A. Hart, X. Xu, R. Legere, and K. Gibble. "A quantum scattering interferometer". *Nature* 446 (2007), 892 (cited on p. 7).

[58] A. S. Mellish, N. Kjærgaard, P. S. Julienne, and A. C. Wilson. "Quantum scattering of distinguishable bosons using an ultracold-atom collider". *Phys. Rev. A* 75 (2007), 020701. DOI: 10.1103/PhysRevA.75.020701 (cited on p. 7).

[59] A. G. Manning. "Foundation experiments in quantum atom optics with ultracold metastable helium". PhD thesis. The Australian National University, 2014 (cited on p. 11).

[60] K. Kornei. "Synopsis: One Very Cold Atom". *APS Physics Focus* (2014) (cited on p. 11).

[61] I. Baumgart, J.-M. Cai, A. Retzker, M. B. Plenio, and C. Wunderlich. "Ultrasensitive Magnetometer using a Single Atom". *Phys. Rev. Lett.* 116 (2016), 240801. DOI: 10.1103/PhysRevLett.116.240801 (cited on p. 11).

[62] M. Schellekens, R. Hoppeler, A. Perrin, J. V. Gomes, D. Boiron, A. Aspect, and C. I. Westbrook. "Hanbury Brown Twiss Effect for Ultracold Quantum Gases". *Science* 310 (2005), 648–651. DOI: 10.1126/science.1118024 (cited on p. 12).

[63] S. S. Hodgman, R. G. Dall, A. G. Manning, K. G. H. Baldwin, and A. G. Truscott. "Direct Measurement of Long-Range Third-Order Coherence in Bose-Einstein Condensates". *Science* 331 (2011), 1046–1049. DOI: 10.1126/science.1198481 (cited on pp. 12, 46).

[64] A. M. Kaufman, B. J. Lester, C. M. Reynolds, M. L. Wall, M. Foss-Feig, K. R. A. Hazzard, A. M. Rey, and C. A. Regal. "Two-particle quantum interference in tunnel-coupled optical tweezers". *Science* 345 (2014), 306–309. DOI: 10.1126/science.1250057 (cited on p. 12).

[65] Dall R. G., Manning A. G., Hodgman S. S., RuGway Wu, Kheruntsyan K. V., and Truscott A. G. "Ideal n-body correlations with massive particles". *Nat Phys* 9 (2013), 341–344. DOI: 10.1038/nphys2632;10.1038/nphys2632 (cited on pp. 12, 46, 62).

[66] G. I. Taylor. "Interference fringes with feeble light". *Proceedings of the Cambridge Philosophical Society*. Vol. 15. 1909, 114–115 (cited on p. 12).

[67] P. Grangier, G. Roger, and A. Aspect. "Experimental Evidence for a Photon Anticorrelation Effect on a Beam Splitter: A New Light on Single-Photon Interferences". *EPL (Europhysics Letters)* 1 (1986), 173 (cited on pp. 12, 72).

[68] J. F. Clauser and A Shimony. "Bell's theorem. Experimental tests and implications". *Reports on Progress in Physics* 41 (1978), 1881 (cited on p. 12).

[69] A. Aspect, P. Grangier, and G. Roger. "Experimental Tests of Realistic Local Theories via Bell's Theorem". *Phys. Rev. Lett.* 47 (1981), 460–463. DOI: 10.1103/PhysRevLett.47.460 (cited on p. 12).

[70] Schlosser Nicolas, Reymond Georges, Protsenko Igor, and Grangier Philippe. "Sub-poissonian loading of single atoms in a microscopic dipole trap". *Nature* 411 (2001). 10.1038/35082512, 1024–1027. DOI: http://dx.doi.org/10.1038/35082512 (cited on p. 12).

[71] S. Kuhr, W. Alt, D. Schrader, M. Müller, V. Gomer, and D. Meschede. "Deterministic Delivery of a Single Atom". *Science* 293 (2001), 278–280. DOI: 10.1126/science.1062725 (cited on p. 12).

[72] R. Dumke, M. Volk, T. Müther, F. B. J. Buchkremer, G. Birkl, and W. Ertmer. "Micro-optical Realization of Arrays of Selectively Addressable Dipole Traps: A Scalable Configuration for Quantum Computation with Atomic Qubits". *Phys. Rev. Lett.* 89 (2002), 097903. DOI: 10.1103/PhysRevLett.89.097903 (cited on p. 12).

[73] D. Schrader, I. Dotsenko, M. Khudaverdyan, Y. Miroshnychenko, A. Rauschenbeutel, and D. Meschede. "Neutral Atom Quantum Register". *Phys. Rev. Lett.* 93 (2004), 150501. DOI: 10.1103/PhysRevLett.93.150501 (cited on p. 12).

[74] Nelson Karl D., Li Xiao, and Weiss David S. "Imaging single atoms in a three-dimensional array". *Nat Phys* 3 (2007). 10.1038/nphys645, 556–560. DOI: http://dx.doi.org/10.1038/nphys645 (cited on p. 12).

[75] Greiner Markus, Mandel Olaf, Esslinger Tilman, Hansch Theodor W., and Bloch Immanuel. "Quantum phase transition from a superfluid to a Mott insulator in a gas of ultracold atoms". *Nature* 415 (2002). 10.1038/415039a, 39–44. DOI: http://dx.doi.org/10.1038/415039a (cited on p. 12).

[76] W. S. Bakr, A. Peng, M. E. Tai, R. Ma, J. Simon, J. I. Gillen, S. Fölling, L. Pollet, and M. Greiner. "Probing the Superfluid–to–Mott Insulator Transition at the Single-Atom Level". *Science* 329 (2010), 547–550. DOI: 10.1126/science.1192368 (cited on p. 12).

[77] J. D. Thompson, T. G. Tiecke, N. P. de Leon, J. Feist, A. V. Akimov, M. Gullans, A. S. Zibrov, V. Vuletić, and M. D. Lukin. "Coupling a Single Trapped Atom to a Nanoscale Optical Cavity". *Science* 340 (2013), 1202–1205. DOI: 10.1126/science.1237125 (cited on p. 12).

[78] A. V. Carpentier, Y. H. Fung, P. Sompet, A. J. Hilliard, T. G. Walker, and M. F. Andersen. "Preparation of a single atom in an optical microtrap". *Laser Physics Letters* 10 (2013), 125501 (cited on p. 12).

[79] A. M. Kaufman, B. J. Lester, and C. A. Regal. "Cooling a Single Atom in an Optical Tweezer to Its Quantum Ground State". *Phys. Rev. X* 2 (2012), 041014. DOI: 10.1103/PhysRevX.2.041014 (cited on p. 12).

[80] J. D. Thompson, T. G. Tiecke, A. S. Zibrov, V. Vuleti ć, and M. D. Lukin. "Coherence and Raman Sideband Cooling of a Single Atom in an Optical Tweezer". *Phys. Rev. Lett.* 110 (2013), 133001. DOI: 10.1103/PhysRevLett.110.133001 (cited on p. 12).

[81] W. Vassen, C. Cohen-Tannoudji, M. Leduc, D. Boiron, C. I. Westbrook, A. Truscott, K. Baldwin, G. Birkl, P. Cancio, and M. Trippenbach. "Cold and trapped metastable noble gases". *Reviews of Modern Physics* 84 (2012), 175–210. DOI: 10.1103/RevModPhys.84.175 (cited on pp. 12, 13, 44, 47, 62, 77).

[82] Jacques V. "Experimental realization of Wheeler's delayed-choice gedanken experiment". *Science* 315 (2007). 10.1126/science.1136303, 966–968. DOI: http://dx.doi.org/10.1126/science.1136303 (cited on pp. 12, 58–60, 70, 72).

[83] A. Einstein, B. Podolsky, and N. Rosen. "Can Quantum-Mechanical Description of Physical Reality Be Considered Complete?" *Phys. Rev.* 47 (1935), 777–780. DOI: 10.1103/PhysRev.47.777 (cited on pp. 12, 16).

[84] S. S. Hodgman, R. G. Dall, L. J. Byron, K. G. H. Baldwin, S. J. Buckman, and A. G. Truscott. "Metastable Helium: A New Determination of the Longest Atomic Excited-State Lifetime". *Phys. Rev. Lett.* 103 (2009), 053002. DOI: 10.1103/PhysRevLett.103.053002 (cited on pp. 13, 62, 74, 77).

[85] A. Browaeys, J. Poupard, A. Robert, S. Nowak, W. Rooijakkers, E. Arimondo, L. Marcassa, D. Boiron, C. I. Westbrook, and A. Aspect. "Two body loss rate in a magneto-optical trap of metastable He". *The European Physical Journal D* 8 (2000), 199–203. DOI: 10.1007/s100530050027 (cited on p. 13).

[86] O. Sirjean, S. Seidelin, J. V. Gomes, D. Boiron, C. I. Westbrook, A. Aspect, and G. V. Shlyapnikov. "Ionization Rates in a Bose-Einstein Condensate of Metastable Helium". *Phys. Rev. Lett.* 89 (2002), 220406. DOI: 10.1103/PhysRevLett.89.220406 (cited on p. 13).

[87] G. B. Partridge, J.-C. Jaskula, M. Bonneau, D. Boiron, and C. I. Westbrook. "Bose-Einstein condensation and spin mixtures of optically trapped metastable helium". *Phys. Rev. A* 81 (2010), 053631. DOI: 10.1103/PhysRevA.81.053631 (cited on pp. 13, 14).

[88] A. Robert, O. Sirjean, A. Browaeys, J. Poupard, S. Nowak, D. Boiron, C. I. Westbrook, and A. Aspect. "A Bose-Einstein Condensate of Metastable Atoms". *Science* 292 (2001), 461–464. DOI: 10.1126/science.1060622 (cited on p. 13).

[89] F. Pereira Dos Santos, J. Léonard, J. Wang, C. J. Barrelet, F. Perales, E. Rasel, C. S. Unnikrishnan, M. Leduc, and C. Cohen-Tannoudji. "Bose-Einstein Condensation of Metastable Helium". *Phys. Rev. Lett.* 86 (2001), 3459–3462. DOI: 10.1103/PhysRevLett.86.3459 (cited on p. 13).

[90] A. S. Tychkov, T. Jeltes, J. M. McNamara, P. J. J. Tol, N. Herschbach, W. Hogervorst, and W. Vassen. "Metastable helium Bose-Einstein condensate with a large number of atoms". *Phys. Rev. A* 73 (2006), 031603. DOI: 10.1103/PhysRevA.73.031603 (cited on p. 13).

[91] R. G. Dall and A. G. Truscott. "Bose-Einstein condensation of metastable helium in a bi-planar quadrupole Ioffe configuration trap". *Opt Commun* 270 (2007), 255–261. DOI: 10.1016/j.optcom.2006.09.031 (cited on pp. 13, 77).

[92] Dall R.G., Hodgman S.S., Manning A.G., Johnsson M.T., Baldwin K.G.H., and Truscott A.G. "Observation of atomic speckle and Hanbury Brown–Twiss correlations in guided matter waves". *Nature Communications* 2 (2011), 291. DOI: http://dx.doi.org/10.1038/ncomms129210.1038/ncomms1292 (cited on pp. 13, 62).

[93] C. J. Dedman, R. G. Dall, L. J. Byron, and A. G. Truscott. "Active cancellation of stray magnetic fields in a Bose-Einstein condensation experiment". *Review of Scientific Instruments* 78 (2007), 024703. DOI: 10.1063/1.2472600 (cited on pp. 13, 62, 77).

[94] J.-C. Jaskula, M. Bonneau, G. B. Partridge, V. Krachmalnicoff, P. Deuar, K. V. Kheruntsyan, A. Aspect, D. Boiron, and C. I. Westbrook. "Sub-Poissonian Number Differences in Four-Wave Mixing of Matter Waves". *Phys. Rev. Lett.* 105 (2010), 190402. DOI: 10.1103/PhysRevLett.105.190402 (cited on pp. 14, 38, 44, 46).

[95] F. Dunning, A. Smith, and R. Stebbings. "Secondary electron ejection from metal surfaces by metastable atoms. I. Measurement of secondary emission coefficients using a crossed beam method". *Journal of Physics B: Atomic and Molecular Physics* 4 (1971), 1683 (cited on p. 15).

[96] R. G. Dall, S. S. Hodgman, M. T. Johnsson, K. G. H. Baldwin, and A. G. Truscott. "Transverse mode imaging of guided matter waves". *Phys. Rev. A* 81 (2010), 011602. DOI: 10.1103/PhysRevA.81.011602 (cited on p. 16).

[97] M. R. Goosen, T. G. Tiecke, W. Vassen, and S. J. J. M. F. Kokkelmans. "Feshbach resonances in ^{3}He*-^{4}He* mixtures". *Phys. Rev. A* 82 (2010), 042713. DOI: 10.1103/PhysRevA.82.042713 (cited on p. 16).

[98] A Perrin, C. M. Savage, D Boiron, V Krachmalnicoff, C. I. Westbrook, and K. V. Kheruntsyan. "Atomic four-wave mixing via condensate collisions". *New Journal of Physics* 10 (2008), 045021 (cited on p. 17).

[99] K. Wright. "Synopsis: Solving Many-Body Problems with a Quantum Microscope". *APS Physics Focus* (2017) (cited on p. 17).

[100] Gwoptics. *Graphics library for illustrations of optics experiments by A. Franzen*. 2006.

[101] E. W. Weisstein. *CRC concise encyclopedia of mathematics*. CRC press, 2002 (cited on p. 24).

[102] M. Amalvict, H. McQueen, and R. Govind. "Absolute Gravity Measurements and Calibration of SG-CT031 at Canberra, 1999-2000". *Journal of the Geodetic Society of Japan* 47 (2001), 410–416 (cited on p. 34).

[103] C. Rose and M. D. Smith. "mathStatica: Mathematical Statistics with Mathematica". *Compstat: Proceedings in Computational Statistics*. Ed. by W. Härdle and B. Rönz. Heidelberg: Physica-Verlag HD, 2002, 437–442. DOI: 10.1007/978-3-642-57489-4_66 (cited on p. 39).

[104] G. K. Campbell, A. E. Leanhardt, J. Mun, M. Boyd, E. W. Streed, W. Ketterle, and D. E. Pritchard. "Photon Recoil Momentum in Dispersive Media". *Phys. Rev. Lett.* 94 (2005), 170403. DOI: 10.1103/PhysRevLett.94.170403 (cited on p. 39).

[105] Schweigler Thomas, Kasper Valentin, Erne Sebastian, Mazets Igor, Rauer Bernhard, Cataldini Federica, Langen Tim, Gasenzer Thomas, Berges Jürgen, and Schmiedmayer Jörg. "Experimental characterization of a quantum many-body system via higher-order correlations". *Nature* 545 (2017), 323–326. DOI: http://dx.doi.org/10.1038/nature2231010.1038/nature22310 (cited on p. 41).

[106] D. S. Simon, G. Jaeger, and A. V. Sergienko. "Ghost Imaging and Related Topics". *Quantum Metrology, Imaging, and Communication*. Cham: Springer International Publishing, 2017, 131–158. DOI: 10.1007/978-3-319-46551-7_6 (cited on p. 44).

[107] B. I. Erkmen and J. H. Shapiro. "Ghost imaging: from quantum to classical to computational". *Adv. Opt. Photon.* 2 (2010), 405–450. DOI: 10.1364/AOP.2.000405 (cited on p. 44).

[108] J. H. Shapiro and R. W. Boyd. "The physics of ghost imaging". *Quantum Information Processing* 11 (2012), 949–993. DOI: 10.1007/s11128-011-0356-5 (cited on p. 44).

[109] P. L. Kapitza and P. A. M. Dirac. "The reflection of electrons from standing light waves". *Mathematical Proceedings of the Cambridge Philosophical Society* 29 (1933), 297–300. DOI: 10.1017/S0305004100011105 (cited on pp. 44, 46).

[110] J. Kofler, M. Singh, M. Ebner, M. Keller, M. Kotyrba, and A. Zeilinger. "Einstein-Podolsky-Rosen correlations from colliding Bose-Einstein condensates". *Physical Review A - Atomic, Molecular, and Optical Physics* 86 (2012), 1–5. DOI: 10.1103/PhysRevA.86.032115 (cited on pp. 44, 46, 56).

[111] B. Jack, J. Leach, J. Romero, S. Franke-Arnold, M. Ritsch-Marte, S. M. Barnett, and M. J. Padgett. "Holographic ghost imaging and the violation of a bell inequality". *Physical Review Letters* 103 (2009), 1–4. DOI: 10.1103/PhysRevLett.103.083602 (cited on pp. 44–46, 56).

[112] T. B. Pittman, Y. H. Shih, D. V. Strekalov, and A. V. Sergienko. "Optical imaging by means of two-photon quantum entanglement". *Phys. Rev. A* 52 (1995), R3429–R3432. DOI: 10.1103/PhysRevA.52.R3429 (cited on p. 44).

[113] D. V. Strekalov, A. V. Sergienko, D. N. Klyshko, and Y. H. Shih. "Observation of Two-Photon "Ghost" Interference and Diffraction". *Phys. Rev. Lett.* 74 (1995), 3600–3603. DOI: 10.1103/PhysRevLett.74.3600 (cited on pp. 44, 46).

[114] D. Klyshko. "Effect of focusing on photon correlation in parametric light scattering". *JETP* 67 (1988), 1131–1135 (cited on p. 44).

[115] A. V. Belinskii and D. N. Klyshko. "Two-photon optics: diffraction, holography, and transformation of two-dimensional signals". *JETP* 78 (1994), 259–262 (cited on p. 44).

[116] B. I. Erkmen. "Computational ghost imaging for remote sensing". *J. Opt. Soc. Am. A* 29 (2012), 782–789. DOI: 10.1364/JOSAA.29.000782 (cited on p. 44).

[117] N. D. Hardy and J. H. Shapiro. "Computational ghost imaging versus imaging laser radar for three-dimensional imaging". *Phys. Rev. A* 87 (2013), 023820. DOI: 10.1103/PhysRevA.87.023820 (cited on p. 44).

[118] S. Yuan, J. Yao, X. Liu, X. Zhou, and Z. Li. "Cryptanalysis and security enhancement of optical cryptography based on computational ghost imaging". *Optics Communications* 365 (2016), 180–185. DOI: 10.1016/j.optcom.2015.12.013 (cited on p. 44).

[119] H. Yu, R. Lu, S. Han, H. Xie, G. Du, T. Xiao, and D. Zhu. "Fourier-transform ghost imaging with hard X rays". *Phys. Rev. Lett.* 117 (2016), 113901. DOI: 10.1103/PhysRevLett.117.113901 (cited on p. 44).

[120] D. Pelliccia, A. Rack, M. Scheel, V. Cantelli, and D. M. Paganin. "Experimental X-ray ghost imaging". *Phys. Rev. Lett.* 117 (2016), 113902. DOI: 10.1103/PhysRevLett.117.113902 (cited on p. 44).

[121] B Sun, M. P. Edgar, R Bowman, L. E. Vittert, S Welsh, a Bowman, and M. J. Padgett. "3D computational imaging with single-pixel detectors." *Science (New York, N.Y.)* 340 (2013), 844–7. DOI: 10.1126/science.1234454 (cited on p. 44).

[122] Ryczkowski Piotr, Barbier Margaux, Friberg Ari T., Dudley John M., and Genty Goëry. "Ghost imaging in the time domain". *Nat Photon* 10 (2016), 167–170. DOI: 10.1038/nphoton.2015.274;10.1038/nphoton.2015.274 (cited on pp. 44, 45).

[123] G. Brida, M. Genovese, and I. Ruo Berchera. "Experimental realization of sub-shot-noise quantum imaging". *Nature Photon.* 4 (2010), 227–230. DOI: 10.1038/nphoton.2010.29 (cited on p. 44).

[124] P. A. Morris, R. S. Aspden, J. E. C. Bell, R. W. Boyd, and M. J. Padgett. "Imaging with a small number of photons." *Nature communications* 6 (2015), 5913. DOI: 10.1038/ncomms6913 (cited on pp. 45, 50).

[125] J. Sprigg, T. Peng, and Y. Shih. "Super-resolution imaging using the spatial-frequency filtered intensity fluctuation correlation". *Scientific Reports* 6 (2016), 38077. DOI: 10.1038/srep38077 (cited on p. 45).

[126] R. S. Bennink, S. J. Bentley, and R. W. Boyd. ""Two-Photon" coincidence imaging with a classical source." *Physical review letters* 89 (2002), 113601. DOI: 10.1103/PhysRevLett.89.113601 (cited on p. 45).

[127] R. S. Bennink, S. J. Bentley, R. W. Boyd, and J. C. Howell. "Quantum and classical coincidence imaging." *Physical review letters* 92 (2004), 033601. DOI: 10.1103/PhysRevLett.92.033601 (cited on p. 45).

[128] F. Ferri, D. Magatti, a. Gatti, M. Bache, E. Brambilla, and L. a. Lugiato. "High-resolution ghost image and ghost diffraction experiments with thermal light". *Physical Review Letters* 94 (2005), 2–5. DOI: 10.1103/PhysRevLett.94.183602 (cited on p. 45).

[129] F. Devaux, P.-A. Moreau, S. Denis, and E. Lantz. "Computational temporal ghost imaging". *Optica* 3 (2016), 698–701. DOI: 10.1364/OPTICA.3.000698 (cited on p. 45).

[130] M. D'Angelo, F. V. Pepe, A. Garuccio, and G. Scarcelli. "Correlation Plenoptic Imaging". *Phys. Rev. Lett.* 116 (2016), 223602. DOI: 10.1103/PhysRevLett.116.223602 (cited on p. 45).

[131] Gong Wenlin and Han Shensheng. "High-resolution far-field ghost imaging via sparsity constraint". 5 (2015), 9280. DOI: http://dx.doi.org/10.1038/srep0928010.1038/srep09280 (cited on p. 45).

[132] P. Zhang, W. Gong, X. Shen, and S. Han. "Correlated imaging through atmospheric turbulence". *Phys. Rev. A* 82 (2010), 033817. DOI: 10.1103/PhysRevA.82.033817 (cited on p. 45).

[133] A. K. Jha, G. A. Tyler, and R. W. Boyd. "Effects of atmospheric turbulence on the entanglement of spatial two-qubit states". *Phys. Rev. A* 81 (2010), 053832. DOI: 10.1103/PhysRevA.81.053832 (cited on p. 45).

[134] P. B. Dixon, G. A. Howland, K. W. C. Chan, C. O'Sullivan-Hale, B. Rodenburg, N. D. Hardy, J. H. Shapiro, D. S. Simon, A. V. Sergienko, R. W. Boyd, and J. C. Howell. "Quantum ghost imaging through turbulence". *Phys. Rev. A* 83 (2011), 051803. DOI: 10.1103/PhysRevA.83.051803 (cited on p. 45).

[135] R. E. Meyers, K. S. Deacon, and Y. Shih. "Turbulence-free ghost imaging". *Applied Physics Letters* 98 (2011), 111115. DOI: 10.1063/1.3567931 (cited on p. 45).

[136] Y. Shih. "The Physics of Turbulence-Free Ghost Imaging". *Technologies* 4 (2016), 39 (cited on p. 45).

[137] M. Yasuda and F. Shimizu. "Observation of two-atom correlation of an ultra-cold neon atomic beam". *Phys. Rev. Lett.* 77 (1996), 3090–3093. DOI: 10.1103/PhysRevLett.77.3090 (cited on p. 46).

[138] Jeltes T., McNamara J. M., Hogervorst W., Vassen W., Krachmalnicoff V., Schellekens M., Perrin A., Chang H., Boiron D., Aspect A., and Westbrook C. I. "Comparison of the Hanbury Brown–Twiss effect for bosons and fermions". *Nature* 445 (2007), 402. DOI: http://dx.doi.org/10.1038/nature05513 (cited on p. 46).

[139] Lewis-Swan R. J. and Kheruntsyan K. V. "Proposal for demonstrating the Hong-Ou-Mandel effect with matter waves". *Nature Commun.* 5 (2014), 3752. DOI: http://dx.doi.org/10.1038/ncomms4752 (cited on p. 46).

[140] Lewis-Swan R. J. and Kheruntsyan K. V. "Proposal for a motional-state Bell inequality test with ultracold atoms". *Phys. Rev. A* 91 (2015), 052114. DOI: 10.1103/PhysRevA.91.052114 (cited on p. 46).

[141] R. Dall and A. Truscott. "Bose–Einstein condensation of metastable helium in a bi-planar quadrupole Ioffe configuration trap". *Optics Communications* 270 (2007), 255–261. DOI: 10.1016/j.optcom.2006.09.031 (cited on pp. 47, 62, 77).

[142] X.-s. Ma, J. Kofler, and A. Zeilinger. "Delayed-choice gedanken experiments and their realizations". *Rev. Mod. Phys.* 88 (2016), 015005. DOI: 10.1103/RevModPhys.88.015005 (cited on pp. 58, 59).

[143] Wheeler J. A. *Mathematical Foundations of Quantum Theory (edited by A. R. Marlow) New York: Academic Press*. 1978 (cited on p. 59).

[144] Bell J. S. *Speakable and Unspeakable in Quantum Mechanics. (Cambridge Univ. Press, Cambridge)*. 1987 (cited on p. 59).

[145] de Broglie L. "Recherches sur la theorie des quanta (Researches on the quantum theory), Thesis (Paris)". *Ann. de Phys.* 3 (1925), 22–128 (cited on p. 59).

[146] Davisson C. and Germer L. H. "Diffraction of electrons by a crystal of nickel". *Phys. Rev.* 30 (1927). 10.1103/PhysRev.30.705, 705–740. DOI: http://dx.doi.org/10.1103/PhysRev.30.705 (cited on p. 59).

[147] Englert B-G. "Fringe visibility and which-way information: An inequality". *Phys. Rev. Lett.* 77 (1996). 10.1103/PhysRevLett.77.2154, 2154–2157. DOI: http://dx.doi.org/10.1103/PhysRevLett.77.2154 (cited on pp. 59, 70, 71).

[148] Hellmuth T., Walther H., Zajonc A., and Schleich W. "Delayed-choice experiments in quantum interference". *Phys. Rev. A* 35 (1987). 10.1103/PhysRevA.35.2532, 2532–2541. DOI: http://dx.doi.org/10.1103/PhysRevA.35.2532 (cited on p. 59).

[149] Alley C. O., Jacubowicz O. G., and Wickes W. C. *Proceedings of the Second International Symposium on the Foundations of Quantum Mechanics, H. Narani, Ed. (Physics Society of Japan, Tokyo)*. 1987 (cited on p. 59).

[150] Baldzuhn J., Mohler E., and Martienssen W. "A wave-particle delayed-choice experiment with a single-photon state". *Zeitschrift für Physik B Condensed Matter* 77 (1989). 10.1007/BF01313681, 347–352. DOI: http://dx.doi.org/10.1007/BF01313681 (cited on p. 59).

[151] Kim Y-H., Yu R., Kulik S. P., Shih Y., and Scully M. O. "Delayed choice quantum eraser". *Phys. Rev. Lett.* 84 (2000). 10.1103/PhysRevLett.84.1, 1–5. DOI: http://dx.doi.org/10.1103/PhysRevLett.84.1 (cited on p. 59).

[152] Ma Xiao-song, Zotter Stefan, Kofler Johannes, Ursin Rupert, Jennewein Thomas, Brukner Caslav, and Zeilinger Anton. "Experimental delayed-choice entanglement swapping". *Nat Phys* 8 (2012). 10.1038/nphys2294, 479–484. DOI: http://dx.doi.org/10.1038/nphys2294 (cited on p. 59).

[153] M. R. Andrews, C. G. Townsend, H.-J. Miesner, D. S. Durfee, D. M. Kurn, and W. Ketterle. "Observation of Interference Between Two Bose Condensates". *Science* 275 (1997), 637–641. DOI: 10.1126/science.275.5300.637 (cited on p. 60).

[154] B. J. Lawson-Daku, R. Asimov, O. Gorceix, C. Miniatura, J. Robert, and J. Baudon. "Delayed choices in atom Stern-Gerlach interferometry". *Phys. Rev. A* 54 (1996), 5042–5047. DOI: 10.1103/PhysRevA.54.5042 (cited on p. 60).

[155] T. Kawai, T. Ebisawa, S. Tasaki, M. Hino, D. Yamazaki, T. Akiyoshi, Y. Matsumoto, N. Achiwa, and Y. Otake. "Realization of a delayed choice experiment using a multilayer cold neutron pulser". *Nuclear Instruments and Methods in Physics Research Section A: Accelerators, Spectrometers, Detectors and Associated Equipment* 410 (1998), 259–263. DOI: 10.1016/S0168-9002(98)00263-0 (cited on p. 60).

[156] M. Schreiber. "Experimentelle Realisierung eines Delayed Choice Experiments mit metastabilen Argonatomen". Theses. Kirchhoff-Institute for Physics, 2008 (cited on p. 60).

[157] G. V. Shlyapnikov, J. T. M. Walraven, U. M. Rahmanov, and M. W. Reynolds. "Decay Kinetics and Bose Condensation in a Gas of Spin-Polarized Triplet Helium". *Phys. Rev. Lett.* 73 (1994), 3247–3250. DOI: 10.1103/PhysRevLett.73.3247 (cited on p. 62).

[158] S. S. Szigeti, J. E. Debs, J. J. Hope, N. P. Robins, and J. D. Close. "Why momentum width matters for atom interferometry with Bragg pulses". *New Journal of Physics* 14 (2012), 023009 (cited on p. 64).

[159] M. Herrero-Collantes and J. C. Garcia-Escartin. "Quantum random number generators". *Rev. Mod. Phys.* 89 (2017), 015004. DOI: 10.1103/RevModPhys.89.015004 (cited on p. 66).

[160] G. Ribordy and O. Guinnard. *Method and apparatus for generating true random numbers by way of a quantum optics process*. US Patent 7,519,641. 2009 (cited on p. 66).

[161] S. Dürr, T. Nonn, and G. Rempe. "Fringe Visibility and Which-Way Information in an Atom Interferometer". *Phys. Rev. Lett.* 81 (1998), 5705–5709. DOI: 10.1103/PhysRevLett.81.5705 (cited on p. 70).

[162] P. D. D. Schwindt, P. G. Kwiat, and B.-G. Englert. "Quantitative wave-particle duality and nonerasing quantum erasure". *Phys. Rev. A* 60 (1999), 4285–4290. DOI: 10.1103/PhysRevA.60.4285 (cited on p. 70).

[163] G. Jaeger, A. Shimony, and L. Vaidman. "Two interferometric complementarities". *Phys. Rev. A* 51 (1995), 54–67. DOI: 10.1103/PhysRevA.51.54 (cited on p. 71).

[164] V. Jacques, E Wu, F. Grosshans, F. m. c. Treussart, P. Grangier, A. Aspect, and J.-F. m. c. Roch. "Delayed-Choice Test of Quantum Complementarity with Interfering Single Photons". *Phys. Rev. Lett.* 100 (2008), 220402. DOI: 10.1103/PhysRevLett.100.220402 (cited on p. 71).

[165] B. M. Henson. "The First Measurement of the 3^3P–2^3P Tune-Out Wavelength in Helium". Honours Thesis. The Australian National University, 2014 (cited on p. 74).

[166] T. Zelevinsky, D. Farkas, and G. Gabrielse. "Precision Measurement of the Three 2^3P_J Helium Fine Structure Intervals". *Phys. Rev. Lett.* 95 (2005), 203001. DOI: 10.1103/PhysRevLett.95.203001 (cited on p. 74).

[167] G Giusfredi, P. C. Pastor, P. D. Natale, D Mazzotti, C de Mauro, L Fallani, G Hagel, V Krachmalnicoff, and M Inguscio. "Present status of the fine-structure frequencies of the 23P helium level". *Can J Phys* 83 (2005), 301–310. DOI: 10.1139/p04-075 (cited on p. 74).

[168] J. S. Borbely, M. C. George, L. D. Lombardi, M. Weel, D. W. Fitzakerley, and E. A. Hessels. "Separated oscillatory-field microwave measurement of the $2\,^3P_1 - 2\,^3P_2$ fine-structure interval of atomic helium". *Phys. Rev. A* 79 (2009), 060503. DOI: 10.1103/PhysRevA.79.060503 (cited on p. 74).

[169] K. Pachucki and V. A. Yerokhin. "Reexamination of the helium fine structure". *Phys. Rev. A* 79 (2009), 062516. DOI: 10.1103/PhysRevA.79.062516 (cited on p. 74).

[170] R. G. Dall, K. G. H. Baldwin, L. J. Byron, and A. G. Truscott. "Experimental Determination of the Helium $2\,^3P_1 - 1^1S_0$ Transition Rate". *Phys. Rev. Lett.* 100 (2008), 023001. DOI: 10.1103/PhysRevLett.100.023001 (cited on pp. 74, 77).

[171] S. S. Hodgman, R. G. Dall, K. G. H. Baldwin, and A. G. Truscott. "Complete ground-state transition rates for the helium $2\,^3P$ manifold". *Phys. Rev. A* 80 (2009), 044501. DOI: 10.1103/PhysRevA.80.044501 (cited on pp. 74, 77).

[172] R. Pohl, A. Antognini, F. Nez, F. D. Amaro, F. Biraben, J. M. R. Cardoso, D. S. Covita, A. Dax, S. Dhawan, L. M. P. Fernandes, et al. "The size of the proton". *Nature* 466 (2010), 213–216. DOI: 10.1038/nature09250 (cited on p. 75).

[173] A. Antognini, F. Nez, K. Schuhmann, F. D. Amaro, F. Biraben, J. M. R. Cardoso, D. S. Covita, A. Dax, S. Dhawan, M. Diepold, L. M. P. Fernandes, et al. "Proton Structure from the Measurement of 2S-2P Transition Frequencies of Muonic Hydrogen". *Science* 339 (2013), 417–420. DOI: 10.1126/science.1230016 (cited on p. 75).

[174] P. J. Mohr, B. N. Taylor, and D. B. Newell. "CODATA recommended values of the fundamental physical constants: 2010*". *Rev. Mod. Phys.* 84 (2012), 1527–1605. DOI: 10.1103/RevModPhys.84.1527 (cited on p. 75).

[175] J. C. Bernauer, P. Achenbach, C. Ayerbe Gayoso, R. Böhm, D. Bosnar, L. Debenjak, M. O. Distler, L. Doria, A. Esser, H. Fonvieille, et al. "High-Precision Determination of the Electric and Magnetic Form Factors of the Proton". *Phys. Rev. Lett.* 105 (2010), 242001. DOI: 10.1103/PhysRevLett.105.242001 (cited on p. 75).

[176] R. Pohl, R. Gilman, G. A. Miller, and K. Pachucki. "Muonic Hydrogen and the Proton Radius Puzzle". *Annu Rev Nucl Sci* 63 (2013), 175–204. DOI: 10.1146/annurev-nucl-102212-170627 (cited on p. 75).

[177] L. J. LeBlanc and J. H. Thywissen. "Species-specific optical lattices". *Phys. Rev. A* 75 (2007), 053612. DOI: 10.1103/PhysRevA.75.053612 (cited on p. 75).

[178] J. Mitroy and L. Tang. "Tune-out wavelengths for metastable helium". *Phys. Rev. A* 88 (2013), 052515. DOI: 10.1103/PhysRevA.88.052515 (cited on pp. 75, 76, 80).

[179] G. W. F. Drake and D. C. Morton. "A Multiplet Table for Neutral Helium (4He I) with Transition Rates". *Astrophys. J., Suppl. Ser.* 170 (2007), 251. DOI: 10.1086/512239 (cited on p. 75).

[180] K. Pachucki and J. Sapirstein. "Relativistic and QED corrections to the polarizability of helium". *Phys. Rev. A* 63 (2000), 012504. DOI: 10.1103/PhysRevA.63.012504 (cited on p. 75).

[181] W. Cencek, K. Szalewicz, and B. Jeziorski. "Breit-Pauli and Direct Perturbation Theory Calculations of Relativistic Helium Polarizability". *Phys. Rev. Lett.* 86 (2001), 5675–5678. DOI: 10.1103/PhysRevLett.86.5675 (cited on p. 75).

[182] G. Łach, B. Jeziorski, and K. Szalewicz. "Radiative Corrections to the Polarizability of Helium". *Phys. Rev. Lett.* 92 (2004), 233001. DOI: 10.1103/PhysRevLett.92.233001 (cited on p. 75).

[183] J. W. Schmidt, R. M. Gavioso, E. F. May, and M. R. Moldover. "Polarizability of Helium and Gas Metrology". *Phys. Rev. Lett.* 98 (2007), 254504. DOI: 10.1103/PhysRevLett.98.254504 (cited on p. 75).

[184] B. Arora, M. S. Safronova, and C. W. Clark. "Tune-out wavelengths of alkali-metal atoms and their applications". *Phys. Rev. A* 84 (2011), 043401. DOI: 10.1103/PhysRevA.84.043401 (cited on p. 76).

[185] J. Jiang, L.-Y. Tang, and J. Mitroy. "Tune-out wavelengths for potassium". *Phys. Rev. A* 87 (2013), 032518. DOI: 10.1103/PhysRevA.87.032518 (cited on p. 76).

[186] Y. Cheng, J. Jiang, and J. Mitroy. "Tune-out wavelengths for the alkaline-earth-metal atoms". *Phys. Rev. A* 88 (2013), 022511. DOI: 10.1103/PhysRevA.88.022511 (cited on p. 76).

[187] C. D. Herold, V. D. Vaidya, X. Li, S. L. Rolston, J. V. Porto, and M. S. Safronova. "Precision Measurement of Transition Matrix Elements via Light Shift Cancellation". *Phys. Rev. Lett.* 109 (2012), 243003. DOI: 10.1103/PhysRevLett.109.243003 (cited on pp. 76, 80).

[188] W. F. Holmgren, R. Trubko, I. Hromada, and A. D. Cronin. "Measurement of a Wavelength of Light for Which the Energy Shift for an Atom Vanishes". *Phys. Rev. Lett.* 109 (2012), 243004. DOI: 10.1103/PhysRevLett.109.243004 (cited on pp. 76, 79, 80).

[189] J. Mitroy, M. S. Safronova, and C. W. Clark. "Theory and applications of atomic and ionic polarizabilities". *Journal of Physics B* 43 (2010), 202001. DOI: 10.1088/0953-4075/43/20/202001 (cited on p. 76).

[190] R. P. M. J. W. Notermans, R. J. Rengelink, K. A. H. van Leeuwen, and W. Vassen. "Magic wavelengths for the $2\,^3S \to 2\,^1S$ transition in helium". *Phys. Rev. A* 90 (2014), 052508. DOI: 10.1103/PhysRevA.90.052508 (cited on p. 76).

[191] P. Meystre. *Atom Optics*. Springer Science & Business Media, 2001 (cited on p. 83).